Student thesis series INES nr 489

Climatic effects of changes in radiative forcing due to clear-cutting in Sweden

Iris Mužić

2019
Department of
Physical Geography and Ecosystem Science
Lund University
Sölvegatan 12
S-223 62 Lund
Sweden

Iris Mužić (2019).
Climatic effects of changes in radiative forcing due to clear-cutting in Sweden
Klimateffekter av förändringar i strålningsdrivningen orsakade av slutavverkning i Sverige
Master degree thesis, 30 credits in *Physical Geography and Ecosystem Science*
Department of Physical Geography and Ecosystem Science, Lund University

Level: Master of Science (MSc)

Course duration: *January* 2019 until *June* 2019

Disclaimer

This document describes work undertaken as part of a program of study at the University of Lund. All views and opinions expressed herein remain the sole responsibility of the author, and do not necessarily represent those of the institute.

Cover photo by Iris Mužić, ICOS station in Hyltemossa

Climatic effects of changes in radiative forcing due to clear-cutting in Sweden

Iris Mužić

Master thesis, 30 credits, in *Physical Geography and Ecosystem Science*

Supervisor
Janne Rinne, Lund University

Co-supervisor
Patrik Vestin, Lund University

Exam committee
Cecilia Akselsson, Lund University
Jutta Holst, Lund University

Acknowledgements

I am grateful to my supervisor Janne Rinne and co-supervisor Patrik Vestin for their constructive suggestions and encouragement throughout my master thesis project. I am also thankful to Michal Heliasz and Tobias Biermann for their advice and guidance in ICOS station Hyltemossa and to Jutta Holst, Maj-Lena Lindersson, Fredrik Lagergren, Anders Lindroth, Jörgen Wallerman and Matthias Peichl for their time and help with the data utilisation. Finally, I thank my family and friends for their care and support.

Abstract

Land cover conversion affects climate by imposing changes in the surface properties and carbon dioxide fluxes. Forest management programs often disregard that modification in surface albedo influences the exchange of energy and climate sensitivity. By taking into account the role of vegetation in shaping the atmospheric circulation, forest harvesting not always leads to the warming of the climate. This study aims to determine the net climatic effect of clear-cutting in high-latitude regions by examining the importance of biogeophysical and biogeochemical climate drivers, albedo and carbon dioxide in Sweden.

Comparative analysis between forest and clear-cut sites on 56°, 60° and 64°N was performed in order to account for different climatic conditions at various latitudes. Data on shortwave incoming radiation, shortwave outgoing radiation and carbon dioxide release from clear-cutting was retrieved from the selected study sites and converted to comparable radiative forcing by albedo change and radiative forcing by carbon dioxide release from clear-cutting.

The findings reveal that the magnitude of the net radiative forcing by clear-cutting differs within high-latitudes. Although with a low confidence level due to the lack of available data, the outcome underlines results from previous studies by indicating that clear-cutting in northern Sweden might induce climate cooling but could also lead to climate warming in southern and central Sweden.

Keywords
Physical Geography and Ecosystem Science, land-cover change, ICOS, albedo, carbon dioxide, radiative forcing, clear-cutting

Table of contents

1. Introduction

Human interference with the climate is observed in several spheres. Fossil fuel combustion and land-use change are the two main sources of perturbation affecting atmospheric greenhouse gas concentration. Moreover, it is unambiguous that the anthropogenic influence has led to the greenhouse effect enhancement since the pre-industrial period (Myhre et al. 2013; IPCC 2014b). Over the last half-century, 18% of the total human-induced carbon dioxide (CO_2) emissions were a result of the land-use change (Quéré et al. 2018). In addition, studies reveal that modifications to the land cover not only change CO_2 fluxes but also have an influence to the surface albedo thereby affecting the exchange of energy (Betts 2000; Bounoua et al. 2002; Myhre and Myhre 2003)

Nowadays, increasing attention is brought to the capacity of vegetation to shape the climate system. On the one hand, vegetation change has an impact on the amount of the absorbed incoming shortwave radiation as well as on the exchanges in heat, moisture and momentum between the Earth's surface and the atmosphere. In this way, it has been shown that the modifications in the vegetation cover affect atmospheric lower boundary conditions and bring about the impact on the climate (Betts 2001). On the other hand, stomatal activity influences evaporation from the leaves as well as carbon uptake by photosynthesis (Bounoua et al. 2002). The efficacy of these plant processes largely depends on the season, species type and on the geographical location (Betts 2000; Betts 2001; Gordon 2008).

A growing amount of literature (Betts 2000; Bounoua et al. 2002; Claussen et al. 2001; Bright et al. 2016) focuses on the relevance of vegetation cover to climate. Some of the studies aim to test the interactions between albedo, soil wetness and surface roughness of different land cover types. In that way, they give an insight into the climate sensitivity to different parameters. Other studies focus more on the coupled effect of different land surface properties and show the influence of the land-cover change to climate on a regional and global level. Since distant climatic disturbance can be altered through the changes in the atmospheric circulation, these studies utilise simulations for comparison of the different radiative forcing drivers. The outcome usually illustrates different responses of the hydrologic cycle and climate to changes in vegetation cover.

Since the reduction of anthropogenic greenhouse gas emissions is a slow process, forest management is seen as an opportunity for faster climate change mitigation. In general, the political imperative, like that of the Paris agreement of the United Nations Framework Convention on Climate Change (UNFCCC 2015), is that forests can counteract climate change because of their ability to remove CO_2 from the atmosphere. Since forests represent global CO_2 sinks, they are believed to slow down the warming induced by the utilisation of fossil fuels (Naudts et al. 2016). The land CO_2 uptake corresponds to 30% of the total emissions over the last half-century period (Quéré et al. 2018). Therefore, afforestation and reforestation are assumed to have a cooling impact on the climate while contributing to the decrease in global temperature (Rost and Mayer 2006).

However, the significance of anthropogenic land cover perturbations on global circulation shows conflicting results (Bounoua et al. 2002). For instance, Naudts et al. (2016) indicate that an increase in the forest area by 10% during the last two and a half centuries in Europe has not resulted in atmospheric CO_2 decrease. More than 85% of the European forests have been put under management so the wood extraction has contributed to the release of carbon stored in the biomass, litter, dead wood and soil carbon pools of the previously unmanaged forests. Conversion of the deciduous forests into coniferous forests resulted in the decrease in evapotranspiration which decreased the thermal heat release from the atmosphere and led to the warming in the central and eastern Europe. Coniferous forests in northern Europe increased albedo due to the sparse forest density and tree canopy. Consequently, forest management and species conversion have contributed to the distinct climatic response based on the investigated area - warming over central Europe and cooling over northern Europe (Betts 2000; Bounoua et al. 2002; Claussen et al. 2001; Bright et al. 2016; Naudts et al. 2016).

Generally, forests feedbacks to the atmosphere impose a challenge to the present climate change studies. First, biogeochemical feedback unveils that forests store carbon by taking up CO_2 from the atmosphere in the process of photosynthesis. This change in biomass thus leads to climate cooling. Second, one biogeophysical feedback suggests that forests have a low albedo and thereby absorbing more shortwave incoming radiation than open treeless landscape. This change in surface structure contributes to climate warming. Third, another biogeophysical feedback of forests suggests that their evapotranspiration increases water vapour in the air. In this way, forests decrease the sensible heat flux which leads to cooling of the atmosphere near the surface. Accordingly, land cover change (e.g. afforestation and deforestation) contributes to the changes in the surface properties and affects atmospheric circulation (Claussen et al. 2001).

As presented, forests can have both warming and cooling effect on climate. Since different feedbacks are interconnected, it is complex to unravel the magnitude of the anthropogenic land cover modifications to climate. In addition, a quantification of the climate sensitivity to land use changes is limited because the plant physiological processes and their adaptations to future climatic conditions are not fully understood (Rost and Mayer 2006).

The objective of this study is to unravel the importance of different forest feedbacks to climate sensitivity in high-latitude regions. The net climatic effect will be investigated by comparing the effect of biogeophysical (albedo change) and biogeochemical (CO_2 release) climate drivers. Here, the evapotranspiration effect will be neglected, because on an annual average in northern latitudes the albedo change outweighs the change in evapotranspiration (Claussen et al. 2001). Also, changes in evapotranspiration are counteracted by changes in sensible heat flux and net radiation. Analysis of the influence of the albedo and CO_2 on climate will be performed by quantifying the amount of the absorbed shortwave incoming radiation (referring to the albedo change) in the forest and clear-cut sites as well as by estimating CO_2 release to the atmosphere by clear-cutting at three different latitudes in Sweden. In this way, it will be possible to investigate the climatic effect of clear-cutting and the differences among its influence along a latitudinal gradient, in the south, central and northern Sweden. The estimated CO_2 release will be translated into an equivalent change in global absorbed radiation in order to perform a comparative analysis of the radiative forcing by albedo change and by CO_2 release.

Even though similar studies aiming to investigate the net climatic forcing have been conducted earlier (Betts 2000; Bounoua et al. 2002; Myhre and Myhre 2003; Chapin et al. 2005; Claussen et al. 2001; Gordon 2008; Luyssaert et al. 2014; Bright et al. 2016; Luyssaert et al. 2018) these were based on model simulations which routinely link the biochemistry of photosynthesis with the biogeophysical regulation of albedo within different global biomes. This study, however, avoids uncertainties unique to specific models and their parameterisations. It is based on available field measurements and thus providing an insight into the climate sensitivity to the selected parameters within the high-latitudes, in Sweden.

The aim of this study is to determine the net climate forcing from the albedo change and CO_2 release by clear-cutting in Sweden. The hypothesis is as follows: In high-latitudes, the cooling effect induced by albedo increase can offset a warming effect by CO_2 release, i.e. high-latitude clear-cutting can reduce climate warming.

2. Background

2.1 Energy balance

Net energy balance at the Earth's surface comprises of the net radiation (R_{net}) components as well as sensible (H), latent (λE) and soil (G) heat fluxes:

$$R_{net} - H - \lambda E - G = 0 \ [W/m^2] \qquad \text{(Eq. 1)}$$

Sensible heat presents the energy stored in a substance that can be derived by cooling it. The latent heat can be extracted through a phase change, so it releases heat when condensation occurs. Heat transport within the ground is mainly through conduction (Houghton 2009; Moene and van Dam 2013).

Net radiation balance (or net radiation) consists of the shortwave incoming radiation (SW_{in}), shortwave outgoing radiation (SW_{out}), longwave incoming radiation (LW_{in}) and longwave outgoing radiation (LW_{out}). It represents the sum of the net shortwave and net longwave radiation fluxes at the surface or at the top of the atmosphere (Monteith and Unsworth 2013):

$$R_{net} = SW_{in} - SW_{out} + LW_{in} - LW_{out} \ [W/m^2] \qquad \text{(Eq. 2)}$$

Shortwave radiation components originate from the Sun. Some of SW_{in} that does not reach the surface is absorbed by the atmosphere. Another part of SW_{in} arrives at the Earth's surface where it is partly absorbed and partly reflected (Kiehl and Trenberth 1997; Houghton 2009). Albedo (α) is the ratio between the reflected energy and the incident energy at the Earth's surface. It is unitless and depends on the surface properties, incoming radiation characteristics as well as on the solar zenith angle (Moene and van Dam 2013):

$$\alpha = \frac{SW_{out}}{SW_{in}} \qquad \text{(Eq. 3)}$$

Longwave radiation components come from the Earth's surface or the atmosphere which in turn radiates thermal energy back to Earth or emits it out to space. LW_{in} and LW_{out} sum up to 235 W/m^2 thereby indicating the presence of the climate equilibrium since the sum of shortwave radiation components that remain in the Earth's system also amounts 235 W/m^2 (Kiehl and Trenberth 1997; Houghton 2009; Moene and van Dam 2013).

Only a small part of the LW_{out} leaves the Earth's system penetrating through the atmosphere (40 W/m^2). It is not absorbed by the atmosphere and re-emitted to the Earth's surface. This is due to the atmospheric selective absorption which strongly depends on wavelength. Hence, the atmosphere is transparent to the shortwave radiation but opaque to most of the longwave radiation. The strongest absorbers of selected wavelength bands are carbon dioxide, water vapour and ozone. Since it is very cold at the levels near the top of the atmosphere (at the heights between 5 and 10 km), these gases emit very little longwave radiation to space. Gaps between the corresponding bands represent little absorption and are thus called atmospheric windows. They occur in the infra-red part of the spectrum where greenhouse gases are transparent for a small portion of LW_{out} (Houghton 2009).

Since longwave radiation fluxes strongly depend on atmospheric temperature, a limited diurnal variation of longwave radiation is a consequence of a relatively small change in temperature in a day and night in comparison to the absolute temperature. The magnitude of longwave radiation is lower in winter than in summer due to the lower atmospheric temperature (Moene and van Dam 2013). Net shortwave radiation, however, depends on sun elevation and albedo and varies considerably throughout both a day and a year. In a clear day, diurnal change between the longwave components is very small in comparison to the net shortwave radiation that nearly follows the shape of the sinusoidal curve. In the overcast day with low clouds, net longwave radiation is about zero so the net radiation during the day almost completely depends on the net shortwave radiation. In the night, the shortwave radiation is zero and the net radiation is almost zero (Monteith and Unsworth 2013).

When perturbations happen in the Earth's system, the energy balance is affected so the Earth responds to the introduced changes by setting up a new climate equilibrium. Climate sensitivity is a change in the annual mean surface temperature as a result of the new radiation balance. The change in temperature is a consequence of some external influence on climate, such as greenhouse effect enhancement or the output of the Sun (Houghton 2009; Roe 2009). Radiative forcing (RF), expressed in W/m^2, is usually used to quantify and compare the anthropogenic and natural climate drivers. It represents a change in net radiation and is calculated either at the tropopause or at the top of the atmosphere (IPCC 2014a). A positive RF tends to increase the temperature, while a negative RF has an opposite effect (Roe 2009). Similarly, perturbations in the Earth's system are often expressed as climate feedbacks which can either be positive or negative. For positive feedbacks, an initial change is enhanced and for negative feedbacks, it is weakened (IPCC 2014a).

2.1.1 Albedo

Land use change affects the exchange of energy in the Earth's system in different ways. Climate impact assessments thus need to take into account the changes in the surface albedo. Generally, the albedo of forested land is lower than that of the open treeless landscape since multiple reflections and scattering of SW_{in} within the canopy reduce the fraction of the upward radiative flux (Betts 2000) as illustrated in Table 1. Radiation can be trapped in multiple layers within the canopy so the albedo decreases with increased vegetation height (Moene and van Dam 2013). The difference between albedo in the forest and in open treeless landscape is most prominent during the snow period. During that time, open areas are completely covered by snow whereas the forests, particularly coniferous forests, expose a darker surface because the snow does not remain on their branches but lies on the forest ground (Betts 2000; Betts 2001).

Table 1. Typical values for albedo for different surface types (Moene and van Dam 2013).

Surface type	Remark	α (-)
Forest	Tropical rain forest	0.07 – 0.15
	Coniferous	0.10 - 0.19
	Deciduous	0.14 – 0.2
Grass		0.15 – 0.30
Soil	Various types	0.10 – 0.35
Snow	Fresh	0.65 – 0.95
	Old	0.45 - 0.65

Anthropogenic influence on albedo is seen in the land cover change and in the CO_2 fertilisation (increased carbon accumulation) which affects the physical characteristics of the vegetation and changes its structure, density and function (Pitman 2003). Changes in albedo throughout a year cause different feedbacks at various land cover types. The complex nature of these changes is usually expressed in feedback loops. Warming in the high-latitude regions causes shrub encroachment and stimulates the forest growth rate (Figure 1). Higher temperatures boost the rate of the photosynthesis which leads to vegetation development. Since trees grow in height with their canopies becoming bigger in size, they expose a darker surface than the open treeless areas. As a result, more incoming radiation is absorbed in the forests which has a heating effect. A low surface albedo in forest areas increases absorbed shortwave radiation (SW_{abs}) thereby providing a warming effect on climate (Claussen et al. 2001).

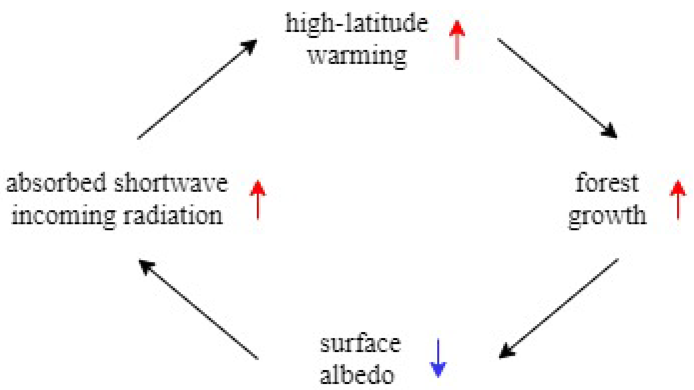

Figure 1. Snow-vegetation albedo feedback (or taiga-tundra feedback).

Coupling latent heat flux and sensible heat flux with albedo increases the complexity of albedo feedbacks to climate. Decreased R_{net} reduces available energy for vegetation growth thereby decreasing both latent and sensible heat fluxes. Lower latent heat flux contributes to less water vapour in the atmosphere and thus, decreased cloudiness and precipitation. Reduced sensible heat flux leads to a decline in both boundary layer heating and in convection. A decrease in cloudiness enhances SW_{in} of an open treeless landscape, however, a high surface albedo again leads to a decrease in SW_{abs} (Pitman 2003). The open treeless landscape has a lower aerodynamic roughness than forests which decreases convective and other dynamic activity that could lead to more rainfall (Houghton 2009). Less precipitation corresponds to reduced soil moisture and reduced vegetation growth. The consequence of this is an increased albedo leading to negative feedback since the SW_{abs} is reduced (Pitman 2003).

2.2 Carbon dioxide

Greenhouse gases absorb thermal radiation from the Earth and can contribute to temperature changes. The most important among the greenhouse gases is water vapour, but human activity has a direct influence on carbon dioxide, methane, nitrous oxide, chlorofluorocarbons and ozone concentrations. Among these, CO_2 has to date contributed approximately 72% of the anthropogenic greenhouse effect enhancement and is the most investigated greenhouse gas (Houghton 2009).

The atmospheric CO_2 concentration is a result of the net land flux, net ocean flux as well as anthropogenic fossil fuel emissions and emissions related to cement production and net land use change (Figure 2). The transport of carbon from soils to the oceans is done by rivers and lakes (Ciais et al. 2013). On a longer time scale, volcanic eruptions (carbon source) and geological weathering thermostat (carbon sink) control the CO_2 concentration. A warmer atmosphere accelerates the rate of silicate and carbonate weathering, leading to an increase in CO_2 uptake (Archer 2010).

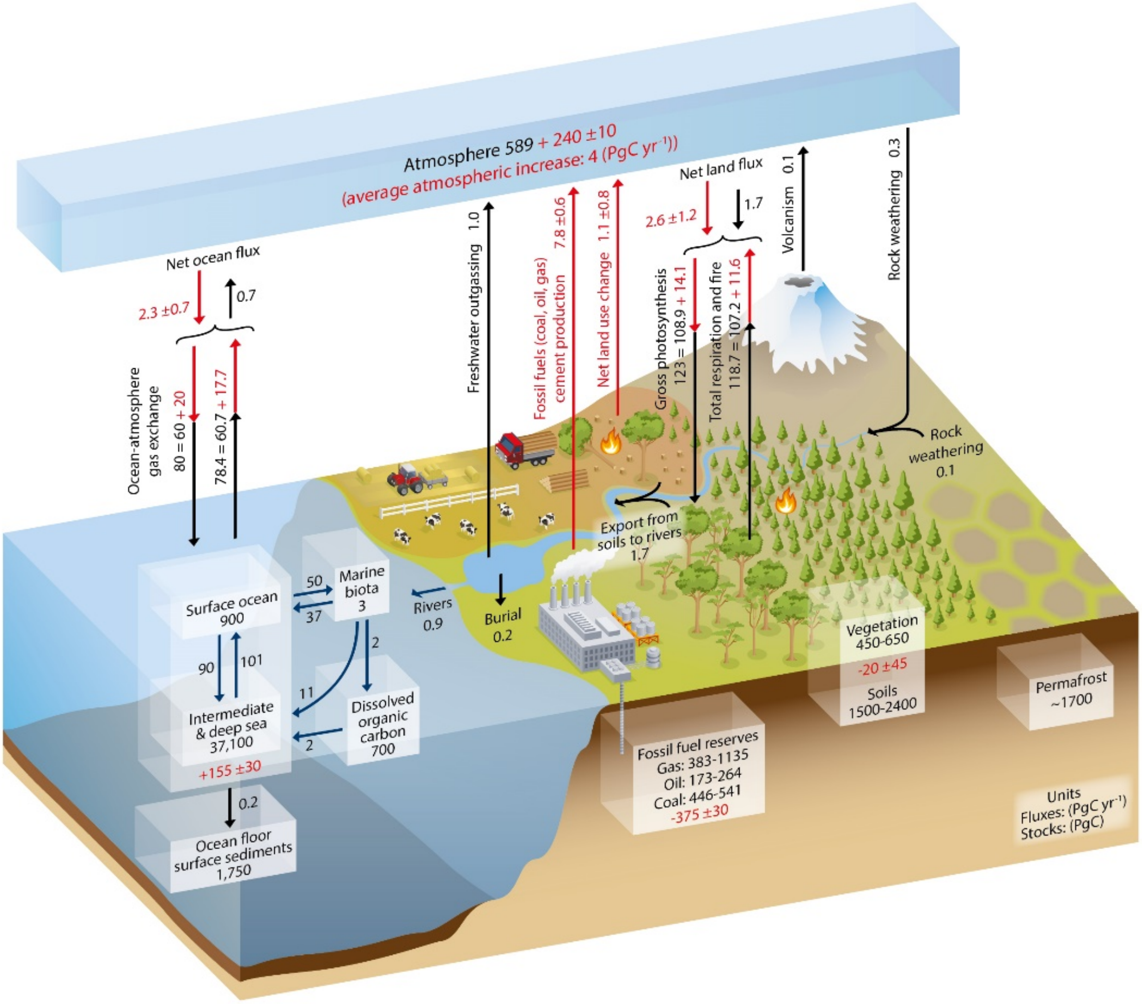

Figure 2. Simplified schematic representation of the global carbon cycle. Black numbers and arrows indicate reservoir mass and exchange fluxes estimated for the time prior to the Industrial Era whereas the red indicators denote cumulative changes of anthropogenic carbon over the Industrial Period 1750–2011 (re-produced from [Ciais et al. 2013] with permission from publisher IPCC).

Through the process of photosynthesis, CO_2 is taken from the atmosphere, converted to carbohydrates and used for the production of organic matter. Respiration is oxidation of carbohydrates which leads to CO_2 release. Carbon is stored in all plant parts, namely in foliage, branches, roots and stem. Decomposition is a process of breaking down organic substances. The decomposition rates of the forests are predominantly influenced by the climatic conditions, substrate availability, vegetation and soil type. Organic matter in the soil is a result of the input of organic matter from vegetation below-ground (root litter) and above-ground (literfall) (Nilsson and Schopfhauser 1995). The anthropogenic disturbance in the CO_2 exchange between the forests and the atmosphere is primarily linked to the extraction of wood for fuel and timber.

2.3 Efficacy of albedo and carbon dioxide forcings

To date, there have been many studies which aimed to compare albedo and CO_2 sequestration potential to investigate the net effect of land cover change to climate (Betts 2000; Bounoua et al. 2002; Myhre and Myhre 2003; Chapin et al. 2005; Claussen et al. 2001; Gordon 2008; Luyssaert et al. 2014; Bright et al. 2016; Luyssaert et al. 2018). These studies accounted for different forest feedbacks and examined both warming and cooling effects in forest ecosystems. Forest areas were presented as carbon sinks demonstrating cooling, which is either enhanced or reduced by warming induced by the albedo effect. For the purpose of comparison between the net effect of radiation and CO_2 in forest areas, albedo and CO_2 climate drivers were transformed to the same units. RF by albedo change ($RF_{\Delta\alpha}$) was in some studies converted to the CO_2 emission equivalents and expressed in, for example, t C/ha (Betts 2000). Similarly, RF by CO_2 release (RF_{co_2}) was in some other studies, converted to W/m^2 where the reference area is either the total area of the Earth or the target area (Bright et al. 2016). Efficacy of climate forcings was in the majority of the studies estimated through model simulations. The common outcome of most of studies was that the biogeophysical forcing (albedo) often outweighed the biogeochemical forcing (CO_2) in high-latitude regions (Betts 2000; Bounoua et al. 2002; Myhre and Myhre 2003; Chapin et al. 2005; Claussen et al. 2001; Gordon 2008; Bright et al. 2016).

2.4 Albedo and carbon dioxide forcings in boreal coniferous forests

Forests cover approximately 31% of the Earth’s surface with boreal forests accounting for about 33% of the global forest area (Keenan et al. 2015). Generally, both satellite-derived and in situ radiation flux measurements show that boreal forests have a lower surface albedo than open treeless areas during the snow season (Gordon 2008). The properties of boreal forests, as well as snowfall, contribute to the strongest albedo decrease with afforestation among all biomes (Betts 2000; Gordon 2008).

The influence of forests on the climate is evident through surface albedo, evapotranspiration and carbon cycle. In comparison to tropical and temperate forests with strong carbon storage in the both above- and below-ground biomass, boreal forests have a lower carbon uptake limited by not only the type of forest but also by temperature, the amount of precipitation and the age of trees (Gordon 2008). However, boreal ecosystems are considered carbon storage because a large amount of carbon remains in the forest soils, permafrost and in wetlands (Gordon 2008). The cold climate and low drained soils in the boreal ecosystems restrict decomposition of detritus leading to the carbon accumulation in the soil (Gower 2003). Furthermore, boreal forests contain about 32% of the global forest stocks of carbon in their biomass and soils (Vestin 2017). The total carbon content per unit area, accounting for both carbon in the vegetation and soil, is about 50% greater in boreal forests than in tropical forests.

Because of the higher temperature and moisture availability, litterfall of the tropical and temperate forest is four to five and two to three times higher than in the boreal forest, respectively (Gower 2003). Drier conditions in the north lead to the weak evaporative cooling in boreal forests. The net forcing to climate by surface albedo, evapotranspiration and carbon cycle in boreal forests is still poorly understood but indicates that warming influenced by low surface albedo may outweigh the importance of carbon sequestration and evaporation (Gordon 2008).

2.5 A life cycle of a managed Swedish forest

The investigated economically managed forests in Hyltemossa, Norunda and Svartberget go through several different stages in their life cycle. In this way, the same area changes surface properties over time as well as imposes both sources and sinks of carbon.

When the forest is young, cleaning ditches and clearing takes place to enhance the growth of the new uniform, coniferous forest. This is done because the deciduous trees, e.g. birch, use the available energy to grow faster than the coniferous trees and thus, might impose negative consequences for the development of the coniferous stand (Bergvik Skog 2019).

While the forest is growing, it takes nutrients and water from the soil and evaporates through stomata. As a result, photosynthesis is enhanced, forest biomass grows and carbon sequestration potential raises. The atmospheric CO_2 is stored in the woody tissues as well as in the constantly produced and gradually decomposed organic matter in litter and soil. The forest soil contains more organic matter and has more litter in comparison to the soil in the clear-cuts owing to the higher nutrient availability (Nilsson and Schopfhauser 1995; Gower 2003). The increased area covered by leaves of the trees provides higher evapotranspiration rates thus leading to an increase in latent heat fluxes and a decrease in sensible heat fluxes in the forest (Mamkin et al. 2019). The surface temperature of the trees is lower than that of the bare soil because trees use available energy for evapotranspiration, rather than for heating of the stems and leaves. Forest gradually increases in height, thereby increasing surface roughness and imposing a darker surface. Correspondingly, surface albedo decreases with the vegetation height because of the multiple reflections of the SW_{in} in the canopy layers (Moene and van Dam 2013). The amount of SW_{abs} in the forest ecosystem roughly increases with the albedo decrease. Consequently, more energy is being trapped in the forest system.

The thinning is performed during the forest growth about one to four times so that finest trees that will later be used as planks can increase in growth and width. The thinning does not decrease the CO_2 uptake (Vesala et al. 2005; Lindroth et al. 2018). Stems, branches and treetops that come from thinnings are often used for paper and bioenergy production. After final thinning, forests are sometimes fertilized in order to maximize the growth of the remaining trees. Nitrogen fertilisation may enhance the carbon sequestration in the forest (Gower 2003; Sathre and Gustavsson 2012).

When boreal forest reaches felling age, the trees are harvested (Bergvik Skog 2019). The management turnover rates in Sweden depend on the region and vary between 60 to 140 years. In order to account for the water management in the soil as well as to protect the bird habitats, some trees are usually left as residuals in the site. Also, some pine trees are left to provide seed. Depending on the use of the harvested stems, branches (and stumps), carbon stored in those tree parts can either instantly be released to the atmosphere in the form of CO_2 through burning or stored in the building structures for a longer time period. The main harvested wood products in Sweden are sawn wood, wood-based panels and paper (Swedish Environmental Protection Agency 2018).

After the harvesting is performed, clear-cut reveals higher albedo, lower evapotranspiration rates and a decrease in SW_{abs}. The reduction in evapotranspiration leads to the raised groundwater table and commonly results in the clear-cuts being wet. In addition, by growing of the grasses, shrubs and small deciduous trees, clear-cuts become drier. Clear-cuts are a CO_2 source because of increased soil respiration and lack of photosynthesis (Gower 2003; Mamkin et al. 2019). The conversion of forests to clear-cuts decreases soil carbon content by approximately 42% and the afforestation increases carbon content in the soil by about 53% (Mamkin et al. 2019). These estimates may vary depending on are the harvest residues left on the clear-cut or some soil scarification method was implemented. The studies on the effect of soil scarification on CO_2 fluxes in a Swedish context revealed that the CO_2 emissions were, on average, lower or equal to the ones at control plots (Vestin 2017).

Finally, after the soil has been prepared for a new forest, forest managers usually plant more seedlings than they aim to harvest, taking into account that not all of the planted trees will reach the felling age (Bergvik Skog 2019).

The highest carbon sequestration in Sweden is in the south-west and the lowest is in the northern parts of the country. The gradient corresponds to the amount of litterfall (Akselsson et al. 2005).

Annual net CO_2 uptake (i.e. net ecosystem productivity, NEP) depends not only on the nutrient availability, soil characteristics and climatic conditions but also on the forest age (Roupsard et al. 2018). Uptake of the CO_2 is not linearly dependent on age and shows a rapid increase at the beginning followed by stabilisation. The stabilisation occurs because the old forests accumulate carbon for a long time and thus contain extensive carbon quantity. Even though they have reduced carbon sequestration rate, they still represent carbon storages (Luyssaert et al. 2008).

3. Methodology

3.1 Study sites description

The study areas chosen for analysis were forests with neighbouring clear-cut/mire sites at three different latitudes in Sweden (Figure 3).

Figure 3. Study site locations (based on data from [ICOS Sweden 2019b]).

In southern Sweden, data from a forest site was taken from the ICOS[1] station Hyltemossa (~53 ha) (ICOS Sweden 2019b) and the nearby clear-cut (~4.8 ha) (Google Earth 2019a) established in 2005. ICOS site Hyltemossa (56°06′N, 13°25′E, 115 m a.s.l.) is situated in northwestern Skåne, a few kilometres south of Perstorp and placed in a predominantly Norway spruce (Picea abies) forest. The trees are on average 19 m high and the forest stand is approximately 35 years old (Table 2). Prevalent soil type at the site is Cambisol (ICOS Sweden 2019b).

In central Sweden, a forest site within ICOS station Norunda and a clear-cut established in 2009 (Vestin 2017) in the close vicinity (~18.5 ha) (Google Earth 2019b) were used for analysis. The Norunda ICOS station (60°05′N, 17°29′E, 46 m a.s.l.) is located about 30 km north of Uppsala surrounded by middle-aged and old (60-110 years) mainly Norway spruce (Picea abies) and Scots pine (Pinus sylvestris) trees with the height of about 25 m. The site is covered by blocks and stones, sandy-loamy tills and soils with a high organic content (ICOS Sweden 2019b).

[1] Integrated Carbon Observation System

In northern Sweden, data from the forest was taken from the ICOS station Svartberget (~1076 ha) and data from a mire was taken from the neighboring ICOS station Degerö (~650 ha). In this study, Degerö was added to simulate an open treeless landscape, as a proxy of a clear-cut, because it provides the only data available in the close vicinity to the Svartberget forest. The albedo of a mire corresponds to the albedo of bare soil, specifically during the presence of a snow cover (Krinner 2003). The Svartberget experimental forests (64°15′N, 19°46′E, 270 m a.s.l.) is about 60 km west of Umeå in a mixed forest consisting of Scots pine (Pinus sylvestris) and Norway spruce (Picea abies). Trees are about 100 years old and 20 m tall. Degerö mire (64°11′N, 19°33′E, 270 m a.s.l.) is situated on a highland between the Umeälven and Vindelälven rivers, approximately 13 km apart from the measurement tower at Svartberget. The geology of both sites comprises of gneiss and moraines (ICOS Sweden 2019b).

Table 2. Study sites land-cover age and height.

Component	Southern Sweden (56°N)		Central Sweden (60°N)		Northern Sweden (64°N)	
	Hyltemossa forest	Hyltemossa clear-cut	Norunda forest	Norunda clear-cut	Svartberget forest	Degerö mire
Age (years)	35	14	60-110	10	100	n. a.
Vegetation height (m)	19	n. a.	25	n. a.	20	n. a.

Data on SW_{in}, SW_{out} and CO_2 were retrieved from three different latitudes in Sweden in order to examine the importance of climate drivers, albedo and CO_2 release, and to compare changes in $RF_{\Delta\alpha}$ and changes in RF_{CO_2}. The reason for the site selection on a latitudinal gradient is because both changes in albedo and CO_2 sequestration depend on meteorological conditions, length of day and snow cover (Moene and van Dam 2013; Roupsard et al. 2018).

In addition to choosing study locations on distinct latitudes, pairs of sites were utilised in southern, central and northern Sweden, respectively. The reason for choosing neighbouring forest and clear-cut areas is the presumption that there is a similarity in meteorological conditions between the sites owing to the short distance between them (Rost and Mayer 2006). Hence, it is assumed that they have the same climatological characteristics, namely, SW_{in}, air temperature, amount of precipitation and wind direction.

The field measurements on radiative fluxes and CO_2 release from harvest were not performed during the NGEM01 course. However, these were explained during the visit to the forest and clear-cut sites in Hyltemossa which took place on the 22nd of March 2019 and were thus described in this report.

3.2 Data on radiation

For the calculation of $RF_{\Delta\alpha}$, only shortwave data was utilised. The same approach was applied by Betts (2000). The mean annual loss of longwave radiative energy from the Earth's system equals the mean net gain from solar radiation. Net shortwave radiation accounts for the total SW_{abs} that is received from space to the Earth's surface. Consequently, RF was calculated for SW_{abs} and not for the R_{net} thereby neglecting the net longwave radiation. Even though the net radiometers utilised in the study sites record both data on net shortwave and net longwave radiation, longwave radiation was disregarded because it originates mostly from the Earth and from the atmosphere thereby remaining in the Earth's energy system. In addition, net longwave radiation shows little variation throughout both a day and a year in comparison to the net shortwave radiation (Moene and van Dam 2013; Monteith and Unsworth 2013).

3.2.1 Field measurements

In all sites, Kipp & Zonen CNR4 net radiometers are utilised for measuring shortwave and longwave radiation flux density (Table 3). They comprise of two pairs of instruments, pyranometer and pyrgeometer, both consisting of upward and downward positioned devices for measuring all four net radiation components (Kipp & Zonen 2019).

Table 3. Instrumentation at study sites.

Component	Southern Sweden (56°N)		Central Sweden (60°N)		Northern Sweden (64°N)	
	Hyltemossa forest	Hyltemossa clear-cut	Norunda forest	Norunda clear-cut	Svartberget forest	Degerö mire
Net radiometer height (m)	50	2-3	50	2-3	50	4

Shortwave radiation is measured with a pyranometer, whereas pyrgeometer is used to measure the longwave radiation (Figure 4). Data used in this study is collected by the pyranometer sensors located below the domes (covers) made of either glass or quartz. Radiation is absorbed at the top of the sensor which causes heating up of the sensor surface. The difference in temperature between the heated top and the cooler bottom indicates the heat flux through the sensors and enables measurements of the radiation input (Moene and van Dam 2013).

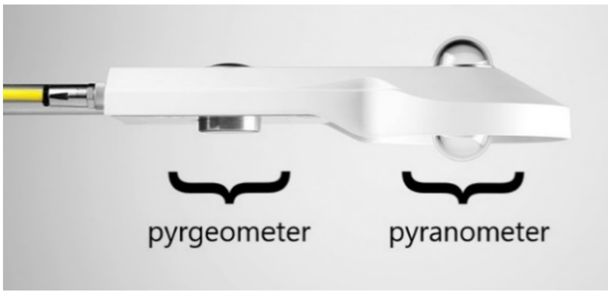

Figure 4. Kipp & Zonen CNR4 net radiometer. Instrument measures shortwave (pyranometer pair) and longwave (pyrgeometer pair) radiation flux (modified from [Kipp & Zonen 2019]).

Some sources of error might occur in measurements of shortwave radiation. In the first place, the instrument must be horizontally aligned. Radiation from the entire hemisphere is collected in the upward pointing sensors whereas about 90% of the radiation is collected from a circle with radius equal to the three times of the height of an instrument in the downward pointing sensors. With this in mind, the location of the instrument is crucial when measuring R_{net} above a heterogeneous surface. Other sources of errors stem from the instruments themselves. For example, since the absorbing surface in pyranometers does not act like a Lambertian surface, it implies different sensitivity for radiation coming from different directions (Moene and van Dam 2013). Another error source in pyranometers refers to the thermal offset owing to the cooler dome than the heated absorbing surface. Consequently, the absorbing surface of the sensor is being cooled specifically during night time, which is why instead of zero flux, the instrument sometimes records negative values. Regular ventilation of the instrument partly overcomes this error because it helps to keep the temperature of the dome similar to the one of the absorbing surface of the sensor (Moene and van Dam 2013). Furthermore, negative radiation values and gaps in data could be a result of low SW_{in} and SW_{out}, power failure, instruments covered by ice and snow, presence of fog between the instrument and the canopy, etc.

3.2.1.1 Forest sites

Measurements of radiation in all ICOS forest sites were recorded as half-hourly averages and taken from the net radiometers installed at 50 m a.g.l. on the tall flux towers (ICOS Sweden 2019a). An example of the flux tower in Hyltemossa is illustrated in Figure 5. The measurements on net radiation are carried out on a boom pointing in a different direction than the others so that no obstacles are positioned in the field of view of the instrument sensors.

Figure 5. Instruments on the tall tower in Hyltemossa. Net radiation is measured on a boom pointing in a different direction than the other instruments. Photo by Iris Mužić.

3.2.1.2 Non-forest sites

In a similar way, but on lower heights, instruments measure exchange in shortwave radiation in Degerö (ICOS Sweden 2019b) and clear-cuts in Hyltemossa and Norunda (Figure 6).


Figure 6. Net radiometer in Hyltemossa clear-cut. Photo by Iris Mužić.

3.3.2 Data download

Data on shortwave radiation for all forest sites and Degerö mire is maintained by ICOS Sweden and was thus downloaded from ICOS Carbon Portal (ICOS Carbon Portal Data 2019). The files in for Hyltemossa, Norunda, Svartberget and Degerö were in ASCII format.

Data on shortwave radiation from clear-cuts in Hyltemossa and Norunda in ASCII format has been provided by researchers at the Department of Physical Geography and Ecosystem Science at Lund University. Data from clear-cuts was pure raw data containing some missing dates and repeated rows.

Only years with available complete annual data on radiation fluxes for both forests and clear-cuts were used in the study. For this reason, three years (2016-2018) of data was available for southern Sweden, five years (2014-2018) in central Sweden and one year (2014) in northern Sweden.

3.3 Data on carbon dioxide

Ideally, data on CO_2 derived from eddy-covariance measurements could have been adopted for calculation of the annual net cumulative CO_2 flux (g $CO_2/m^2/yr$). However, the readily available data on CO_2 flux from clear-cuts in Hyltemossa and Norunda did not correspond to the same time periods as data obtained for radiation.

Since the amount of CO_2 emitted by clear-cutting equals to the atmospheric CO_2 that was utilised by the tree through growing (Gower 2003), data on the volume of harvested wood from clear-cut provided by the forest owners in Hyltemossa was used to calculate how much carbon was released into the atmosphere by forest harvesting in the present day clear-cut in Hyltemossa. The forest in Norunda is maintained by multiple forest owners who performed harvesting. For that reason, in order to obtain required data on amount of carbon stored in the trees in Norunda within the time frame of the thesis project, an estimated amount of above-ground carbon (in the standing biomass) in Norunda forest site (in kilograms of carbon per square meter) given by Håkansson and Körling (2002) was utilised. Similarly, the amount of above-ground biomass in Svartberget forest (in tonnes of dry matter per hectare) was taken from Wallerman et al. (2018),

Generally, root biomass is estimated to be about 20% of the above-ground forest carbon stock (Marklund 1988). A few studies on afforestation, which implies lower carbon content in the root biomass than it is in the unmanaged forests, suggest that about 80% of the total carbon storage of the tree is in the above-ground components thereby excluding the parts in the soil (Nilsson and Schopfhauser 1995; Gower 2003). These estimates might, however, vary depending on the considered biome, nutrient availability, soil characteristics, climatic conditions, etc. In this study, the above-ground carbon stock was assumed to correspond to 80% of the total carbon in the tree because the investigated forests in Sweden are actively managed. Hence, the calculated amount of CO_2 release from clear-cutting which corresponds only to above-ground carbon stock of the trees was divided by 0.8. In this way, RF_{CO_2} accounted for the total amount of carbon in the tree, stored in harvested above-ground components and below-ground components. By including the below-ground carbon stock of the tree in the RF_{CO_2} calculation, not only instant CO_2 release by clear-cutting was accounted for, but also part of the CO_2 emission from the soil after clear-cutting. However, gradual changes in the soil carbon stock after clear-cutting e.g. reduced litter inputs to the soil, increased decomposition rate of older material in soil and movement of carbon from upper to lower soil layers in the clear-cut (Sathre and Gustavsson 2012) were neglected. Therefore, the resulting RF_{CO_2}shows how much warming causes a release of CO_2 from the entire carbon stock of the tree due to clear-cutting (Figure 7). Here, the assumption is that all carbon previously stored in the tree is released to the atmosphere in a relatively short time.

In reality, not all CO_2 from the forest biomass is released shortly after harvesting. Some of the harvested biomass is, for instance, used as a building material and not subject to combustion. Other parts of the tree stems are used for relatively short-lived wood products while tree tops and branches are often utilised for bioenergy production where the CO_2 is quickly released to the atmosphere through burning. Stumps are sometimes also harvested for bioenergy production although this takes place on very small areas annually (Vestin, 2017). More commonly, the stumps are left at the site and gradually decomposed. In comparison to logs and stumps, fine roots and needles decay more rapidly (Sathre and Gustavsson 2012) if left on site. However, a complete life-cycle analysis of the residues and wood products after harvesting is outside of the scope of this study.

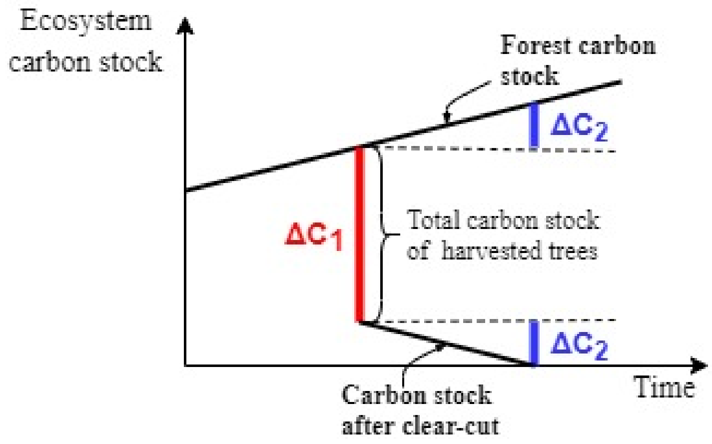

Figure 7. A simplified illustration of the change in the ecosystem carbon stock induced by forest harvesting. In this study, only change in the carbon stock due to the release of CO_2 in a relatively short time by clear-cutting (ΔC_1) was considered. The effect of changes in the forest and clear-cut carbon stocks (CO_2 uptake and release) by time (ΔC_2) was neglected.

3.3.1 Field measurements

There are two types of tree biomass estimation in the field, destructive and a non-destructive method. Data on above-ground biomass and forest carbon stocks used in this study was collected from the destructive (harvest method). It is based on measurements of the weight of the tree trunk, leaves and branches of harvested trees before and after they have been oven dried. Harvest method is usually applied on a smaller scale in order to develop biomass equations and estimate biomass in the larger areas. Biomass is assessed using allometric equations for single species or a mixture of species referring to the relationship among the breast height diameter, crown diameter, tree trunk height, total tree height, etc. (Vashum 2012).

3.4 Data analysis

3.4.1 Radiative flux

3.4.1.1 Mean daily albedo calculation

The calculation of albedo for all half-hourly measurements was performed in MATLAB using the equation Eq. 3. Every day Sun passes over different zenith and azimuth angles. When the solar altitude is low, the solar zenith angle is high and that causes higher albedo values (Figure 8). This happens because the SW_{in} in the morning and late afternoon reflects from the top of the leaves and does not go through the vegetation. On the contrary, around midday time, SW_{in} is trapped in the vegetation which causes multiple reflections and slightly lowers the albedo. Diurnal cycle of a clear, sunny, summer day is evident, with the lowest albedo values being during midday when the SW_{in} and the SW_{out} are the highest. On a cloudy, snowy, winter day, the albedo varies a lot due to the large measurement uncertainties in SW_{in} and SW_{out} because of their low values (Moene and van Dam 2013).

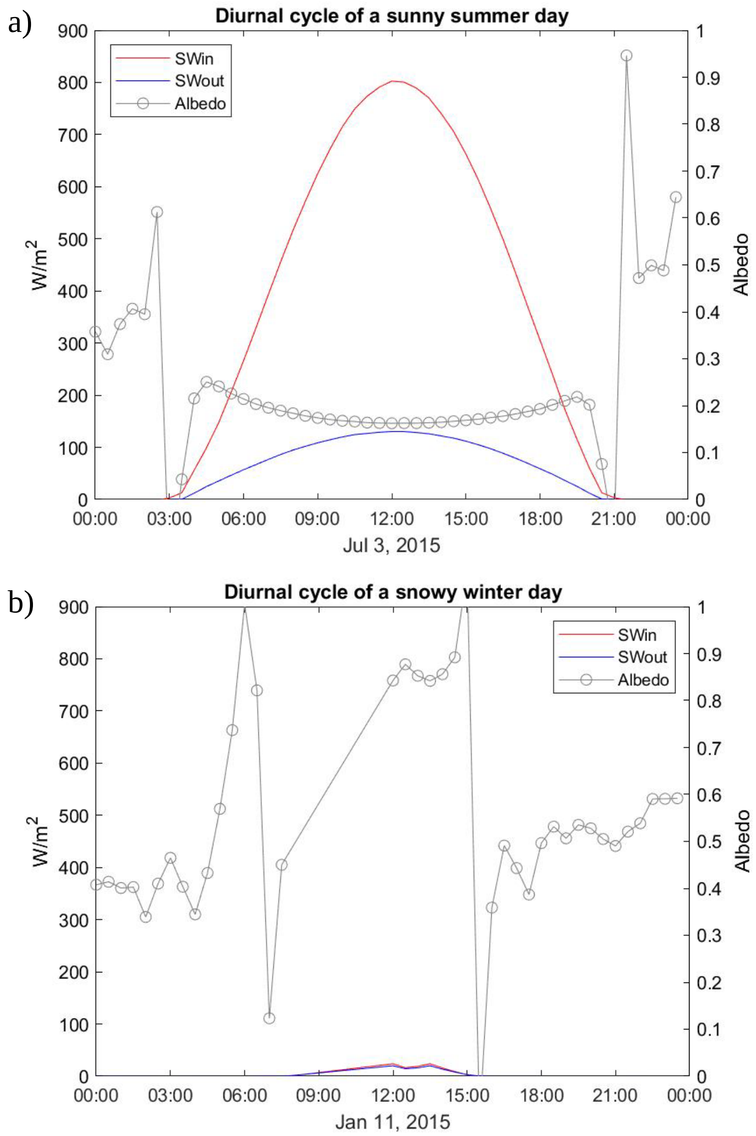

Figure 8. Diurnal cycle of albedo and SW_{in} and SW_{out} in Norunda clear-cut in a) summer day and b) winter day in 2015. The example b) illustrates that there might only be a few measurements within the whole day which could be used for mean daily albedo calculation during winter.

Only appropriate albedo values were extracted from the dataset for the calculation of mean daily albedo. For instance, it is possible to use only half-hourly measurements on shortwave radiation for midday hours, for instance between 10:00 and 14:00 when the Sun's elevation is the highest, the solar zenith angle is low and the albedo values are constant (Moene and van Dam 2013). However, following this methodology, the differences in the length of the daylight hours in the south and in the north of Sweden as well as between winter and summer would not be considered so the resulting average daily albedo might not be representative for the selected sites. Another technique might have been to omit the non-valid albedo measurements where albedo values are not in the range between 0 and 1 as well as those when SW_{in} and/or SW_{out} are negative. However, this approach would not account for the data on albedo when the absolute values of SW_{in} or SW_{out} are very low or for the disturbances such as, for example, power failure, snow and ice covering the instrument or fog. As a result, the extraction of required albedo measurements for the mean daily albedo calculation was based on predefined SW_{in} threshold. The threshold set for all sites was 50 W/m^2. In this way, half-hourly measurements were separated in above 50 W/m^2 and below 50 W/m^2 data on SW_{in} (Figure 9).

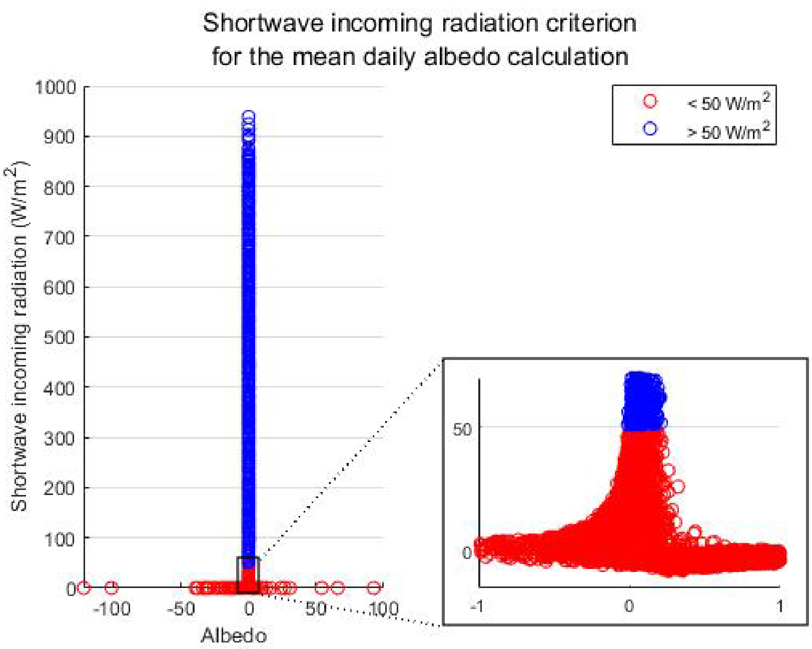

Figure 9. Shortwave incoming radiation above 50 W/m^2 was used as a criterion for the mean daily albedo calculation. The example shown is from Hyltemossa forest in 2017.

Mean daily albedo was calculated in MATLAB. Only daily average was used for further calculation because albedo does not show a lot of variation throughout the day. Data in clear-cut sites was missing some half-hourly shortwave radiation measurements. Hence, mean daily albedo was calculated from the available data and missing values were interpolated. Gap-filling of missing data was done on daily average basis, using a shape-preserving piecewise cubic interpolation (pchip2) of at least four average daily albedo neighbouring values. Interpolation methods that require minimum two embracing points, as for instance linear, were not picked since these only account for two neighbouring values and do not fill missing data in the beginning or at the end of the dataset. Even though both pchip and spline interpolation techniques require at least four points, pchip showed better performance because it does not overshoot as freely as a spline (Figure 10).

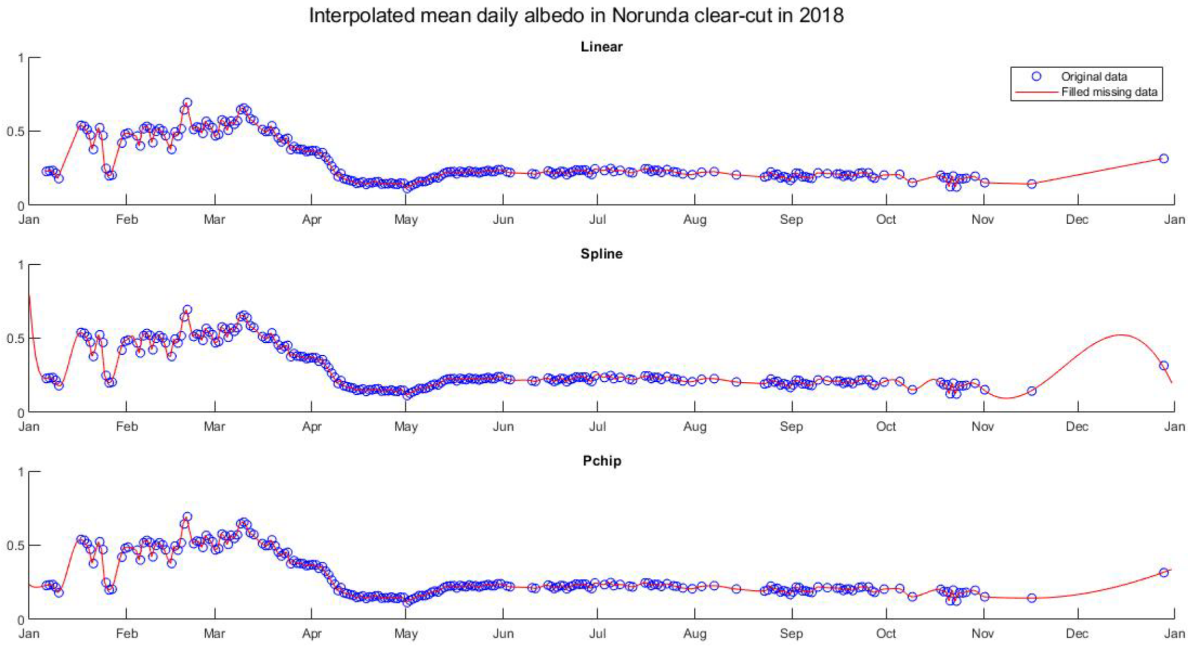

Figure 10. Comparison of the three commonly used interpolation methods. The notable difference among the methods could be detected in months with sparse data (Jan, Nov, Dec).

3.4.1.2 Mean annual absorbed radiation calculation

In order to account for the same SW_{in} in study site pairs, SW_{in} recorded in ICOS forest stations was used for calculation of mean daily absorbed radiation in both forest and clear-cut sites. This approach corresponds to the assumption that there is the same SW_{in} in the neighbouring study locations.

Mean daily shortwave incoming radiation was calculated as a mean of all SW_{in} measurements during the whole diurnal cycle without gap-filling on 30 min basis. Given that length of the day differs among latitudes and between winter and summer, in this way, all variations within the day were considered for the calculation of the mean daily absorbed radiation.

The calculation of mean daily absorbed shortwave radiation was performed in MATLAB using the equation derived from the Eq. 3:

$$SW_{abs} = (1 - \alpha) \times SW_{in} \; [W/m^2] \qquad \text{(Eq. 4)}$$

where SW_{abs} is the mean daily absorbed shortwave radiation, α is the interpolated mean daily albedo and SW_{in} is the mean daily shortwave incoming radiation in the forest study site.

Mean annual absorbed radiation was then calculated as an average of the mean daily absorbed radiation data.

3.4.1.3 Radiative forcing calculation

The calculation of the radiative forcing by albedo change was performed in Excel. The annual mean RF at each of the study site pairs can be calculated using:

$$RF_{\Delta\alpha} = \frac{SW_{abs}^{clear-cut} - SW_{abs}^{forest}}{Area^{Earth}} \ [W/m_{Earth}^2] \quad \text{(Eq. 5)}$$

where $RF_{\Delta\alpha}$ is the radiative forcing by albedo change calculated as a difference between SW_{abs} in a clear-cut and forest and divided by the total area of the Earth ($Area^{Earth}$). The surface area of the Earth amounts 1.5×10^{14} m^2 (Scientific American 1999). This equation is utilised because it provides the effect of albedo change due to clear-cutting.

3.4.2 Carbon dioxide emission

3.4.2.1 Hyltemossa clear-cut

The total amount of harvested wood provided by the forest owners in Hyltemossa is 545.82 m^3f ub (cubic meters under bark) and 1211.80 $m^3$to ub (cubic meters top measurement under bark). These units were converted to forest cubic meters[2], m^3sk using the table provided by SkogsSverige (2016) and summed up. Total mass m of the carbon in the harvested wood in the whole target area (per m^2) was derived from the equation:

$$m = \frac{\rho \times V}{Area} \ [t\ C/m^2] \quad \text{(Eq. 6)}$$

where ρ is the density of carbon in the total above-ground biomass of European forests (soil carbon fixation in the forest is excluded), amounting 0.3 t C/m^3 (Nilsson and Schopfhauser 1995), V is the volume of harvested wood and Area is the clear-cut area. According to Nilsson and Schopfhauser (1995), no assessment on the carbon sequestration potential per m^3 on the subregional level has been made available.

Calculation of the change in the CO_2 atmospheric concentration due to forest harvesting was based on the estimate that 2.12 Gt C stands for 1 ppm of atmospheric CO_2 (Quéré et al. 2018).

Radiative forcing by CO_2 release for the whole forest biomass was then calculated from the following equation derived from Betts (2000):

[2] Forest cubic meters account for the tree trunk volume including top and bark above the stubble cut (SkogsSverige 2016).

$$RF_{co_2} = \left(5.35ln\left(1 + \frac{\Delta C}{C_0}\right)\right)/0.8\ [W/m^2_{Earth}] \quad \text{(Eq. 7)}$$

where RF_{co_2} is radiative forcing by CO_2 release, ΔC is a change in the CO_2 atmospheric concentration and C_0 is the reference concentration. The reference concentration used was 411.97 ppm representing an average CO_2 concentration in March 2019 (Earth's CO_2 2019). The reason for dividing the equation provided by Betts (2000) by 0.8 is because RF_{co_2} accounts for total carbon stock in the tree.

3.4.2.2 Norunda forest

Since there was no data on the harvest of the clear-cut available, existing standing above-ground biomass in Norunda was used. An estimated amount of above-ground carbon in Norunda forest is 10.52 kg C/m^2 with an uncertainty of 18% (Håkansson and Körling 2002). The amount was expressed in t C/m^2 and converted to Gt C and divided by 2.12 to obtain the change in the CO_2 atmospheric concentration induced by forest harvesting. RF_{co_2} was then determined using Eq. 7.

3.4.2.3 Svartberget forest

Utilising a mire instead of a clear-cut in the north of Sweden did not have implications on the amount of CO_2 emission by clear-cutting since this was estimated based on the assumption that the present day trees in Svartberget forest are harvested. The mean above-ground biomass in Svartberget forest used to simulate yield of harvesting is 111.49 t dry weight/ha (Wallerman et al. 2018). Carbon concentration of tree components corresponds to 50% of the dry biomass (Vashum 2012). Hence, the provided amount was divided by 2 to get the total mass of the above-ground carbon in the whole target area (in t C/m^2). The following procedure was then the same as in the case of Norunda.

3.4.3 Net radiative forcing confidence interval calculation

After a net radiative forcing, RF_{net} was calculated as a difference between the $RF_{\Delta\alpha}$ and RF_{co_2}, as the last step, standard error of the mean was determined using:

$$SEM = \frac{\sigma}{\sqrt{N}} \quad \text{(Eq. 8)}$$

where SEM is a standard error of the mean, σ is a standard deviation of RF_{net} and N is the number of considered years in the study sites. In order to account for a confidence level of 95% (or statistical significance of 5%) which is typically used for data representation, SEM was then multiplied by 1.96.

4. Results

4.1 Radiative flux

Annual variability in albedo and SW_{in} across different latitudes is illustrated in Figure 11. Mean daily albedo at clear-cuts is higher than the albedo of forests throughout the whole year. The annual pattern of SW_{in} is reversed to the one of albedo with the highest values in the summer months and the lowest in winter. In the south, SW_{in} varied considerably within the whole year. In the north, however, the biggest variation in SW_{in} was during summer months. Higher sun elevation angles and longer daylight hours enhance mean daily SW_{in} during summer months in the northern high-latitudes which resulted in the highest daily average SW_{in} values being recorded in Svartberget.

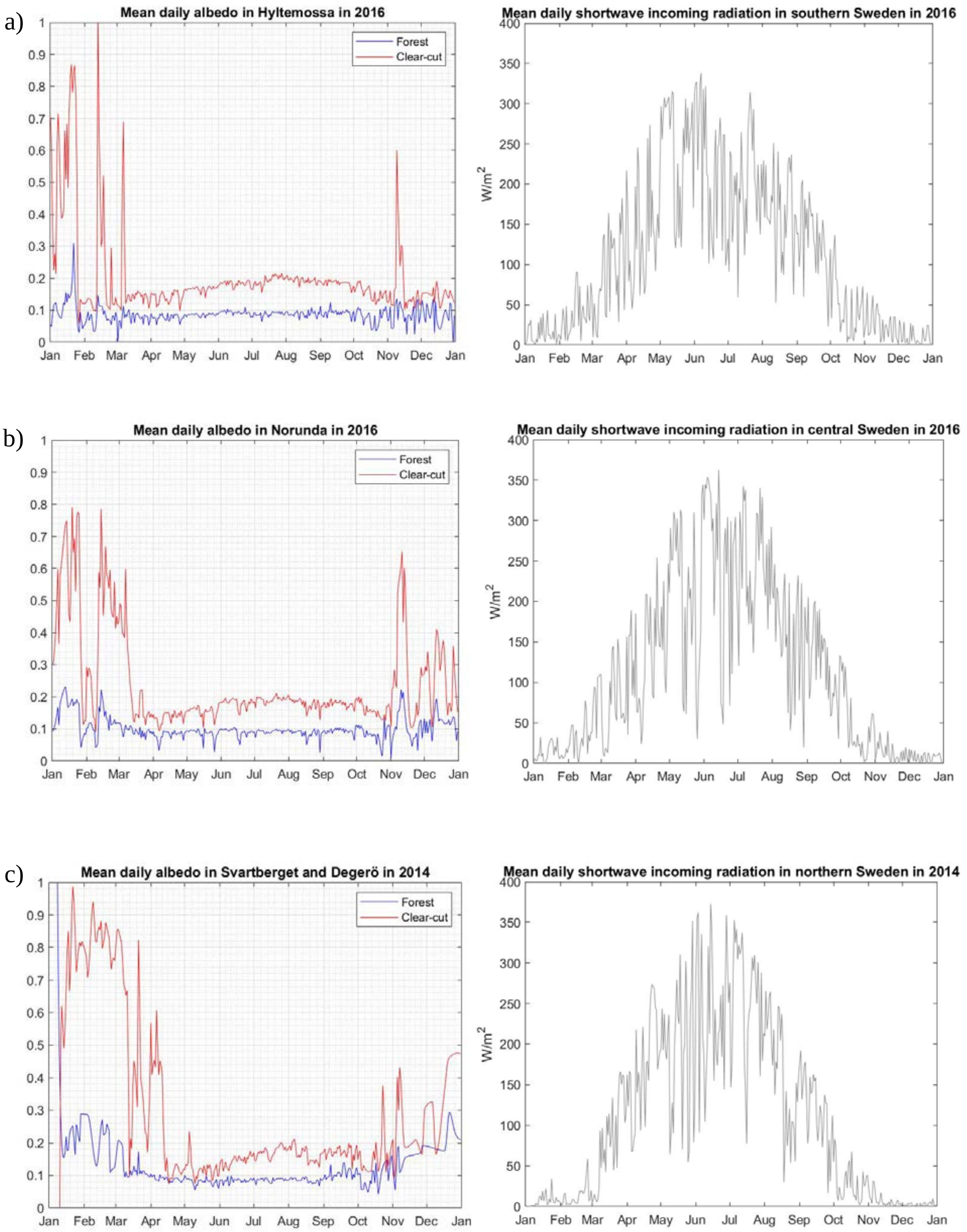

Figure 11. Comparison between the annual pattern of mean daily albedo and mean daily SW_{in} in a) Hyltemossa in 2016, b) Norunda in 2016 and c) Svartberget and Degerö in 2014.

During the investigated period, the mean annual SW_{in} was highest in Norunda and lowest in Svartberget (Table 4). Overall, the highest SW_{in} was recorded in Norunda in 2018 and the lowest in Svartberget in 2014. The mean annual albedo value across the examined periods of a clear-cut site was higher than the one of a forest site by 57-59% depending on the latitude. The largest difference between the mean annual clear-cut and forest albedo was in the north. There was a larger variation in albedo in clear-cuts (0.20 – 0.30) than in forests (0.08-0.13) among various years. In addition, mean annual albedo increases with increased latitude in both forest and clear-cut sites.

Table 4. Mean annual SW_{in} and albedo in study locations.

	Mean annual SW_{in} (W/m^2)	Mean annual α (-)	
Southern Sweden	Hyltemossa	Hyltemossa forest	Hyltemossa clear-cut
2016	110.0	0.09	0.20
2017	100.8	0.08	0.20
2018	121.0	0.09	0.21
Central Sweden	Norunda	Norunda forest	Norunda clear-cut
2014	113.0	0.10	0.21
2015	112.6	0.10	0.23
2016	111.6	0.10	0.24
2017	110.7	0.10	0.22
2018	126.3	0.10	0.26
Northern Sweden	Svartberget	Svartberget forest	Degerö mire
2014	107.9	0.13	0.30

Winter albedo was generally higher than summer albedo in all locations (Table 5). The difference between winter and summer albedo was the largest in the north. Also, the highest mean albedo values were recorded during winter months in the north of Sweden, 0.21 and 0.79 in Svartberget and Degerö, respectively.

Table 5. Mean winter (January and February) and summer (July and August) albedo.

	Mean α (-)			
	Winter	Summer	Winter	Summer
Southern Sweden	Hyltemossa forest		Hyltemossa clear-cut	
2016	0.10	0.09	0.36	0.19
2017	0.09	0.09	0.27	0.20
2018	0.09	0.09	0.32	0.18
Central Sweden	Norunda forest		Norunda clear-cut	
2014	0.11	0.10	0.39	0.18
2015	0.14	0.09	0.54	0.18
2016	0.14	0.09	0.47	0.18
2017	0.11	0.10	0.34	0.21
2018	0.14	0.09	0.42	0.22
Northern Sweden	Svartberget forest		Degerö mire	
2014	0.21	0.09	0.79	0.17

Mean annual SW_{abs} was always higher in forest sites than in clear-cuts (Table 6). The largest mean annual difference in SW_{abs} (ΔSW_{abs}) between forests and clear-cuts was in Norunda sites in 2018 (17.5 W/m^2).

Table 6. Mean annual absorbed radiation in study sites.

	Mean annual SW_{abs} (W/m^2)		Mean annual ΔSW_{abs} (W/m^2)	$\frac{\text{mean annual } SW_{abs}^{clear-cut}}{\text{mean annual } SW_{abs}^{forest}}$ (%)
Southern Sweden	Hyltemossa forest	Hyltemossa clear-cut	Hyltemossa	
2016	100.1	89.9	10.2	89.8
2017	92.1	81.1	11.0	88.0
2018	109.6	97.5	12.0	89.0
Central Sweden	Norunda forest	Norunda clear-cut	Norunda	
2014	102.2	92.5	9.6	90.6
2015	101.8	91.8	9.9	90.2
2016	101.0	90.2	10.8	89.3
2017	100.1	89.0	11.1	88.9
2018	113.8	96.3	17.5	84.6
Northern Sweden	Svartberget forest	Degerö mire	Svartberget and Degerö	
2014	97.8	87.7	10.1	89.7

The cumulative sum of the mean daily SW_{abs} was calculated for both forest and clear-cut sites to illustrate the difference in their annual pattern throughout the year. As expected from Figure 11. and Eq. 4, the results show that cumulative sum of the mean daily SW_{abs} was higher in the forest than in the clear-cut throughout the whole year, in all study site pairs, starting to diverge already during winter months. An example of a study site pair is given in Figure 12.

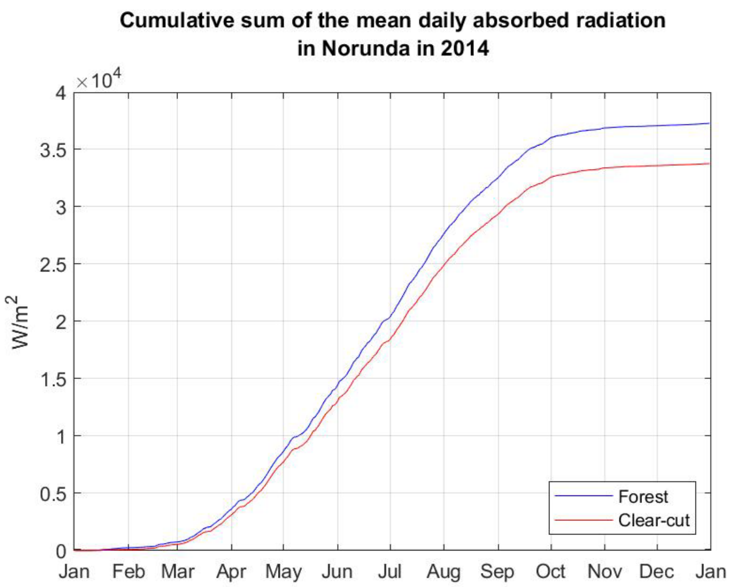

Figure 12. Cumulative sum of the mean daily absorbed radiation for the forest and for the clear-cut site in Norunda in 2014.

The cumulative difference between the mean daily SW_{abs} in forests and clear-cuts was calculated by subtracting the cumulative sum of the mean daily SW_{abs} in the clear-cut from the one of the forest to examine how SW_{abs} components, SW_{in} and albedo, shape the magnitude of SW_{abs}. The cumulative difference between the mean daily SW_{abs} in forests and clear-cuts increases by time at all examined latitudes (Figure 13).

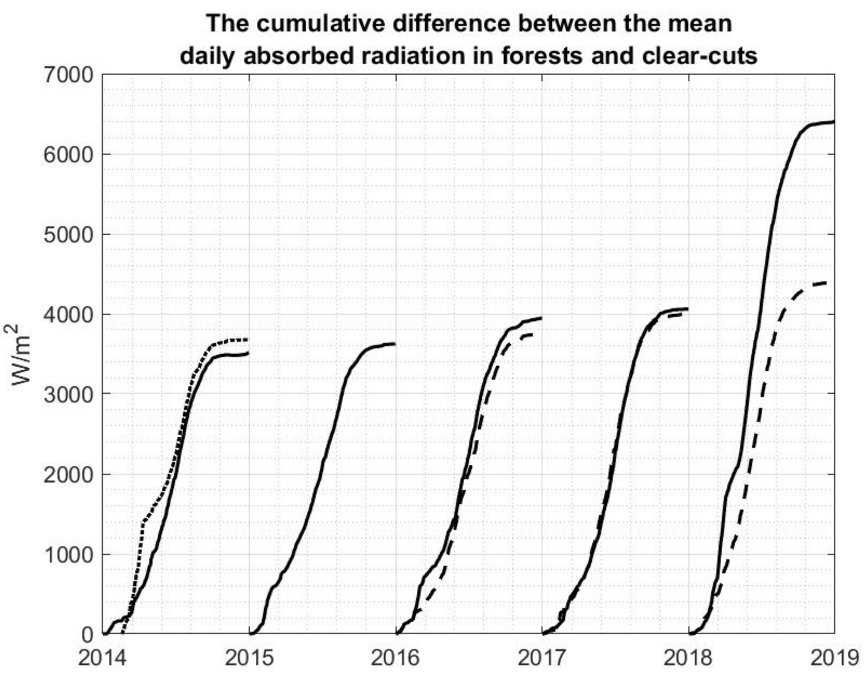

Figure 13. The cumulative difference between the mean daily SW_{abs} in forests and clear-cuts in Hyltemossa (dashed line), Norunda (solid line) and Svartberget (dotted line).

Since the cumulative difference between the mean daily SW_{abs} in forests and clear-cuts shows the largest disparity between the Hyltemossa and Norunda sites in 2018 (Figure 13), the annual pattern of the mean daily albedo and mean daily SW_{in} are compared in Figure 14.

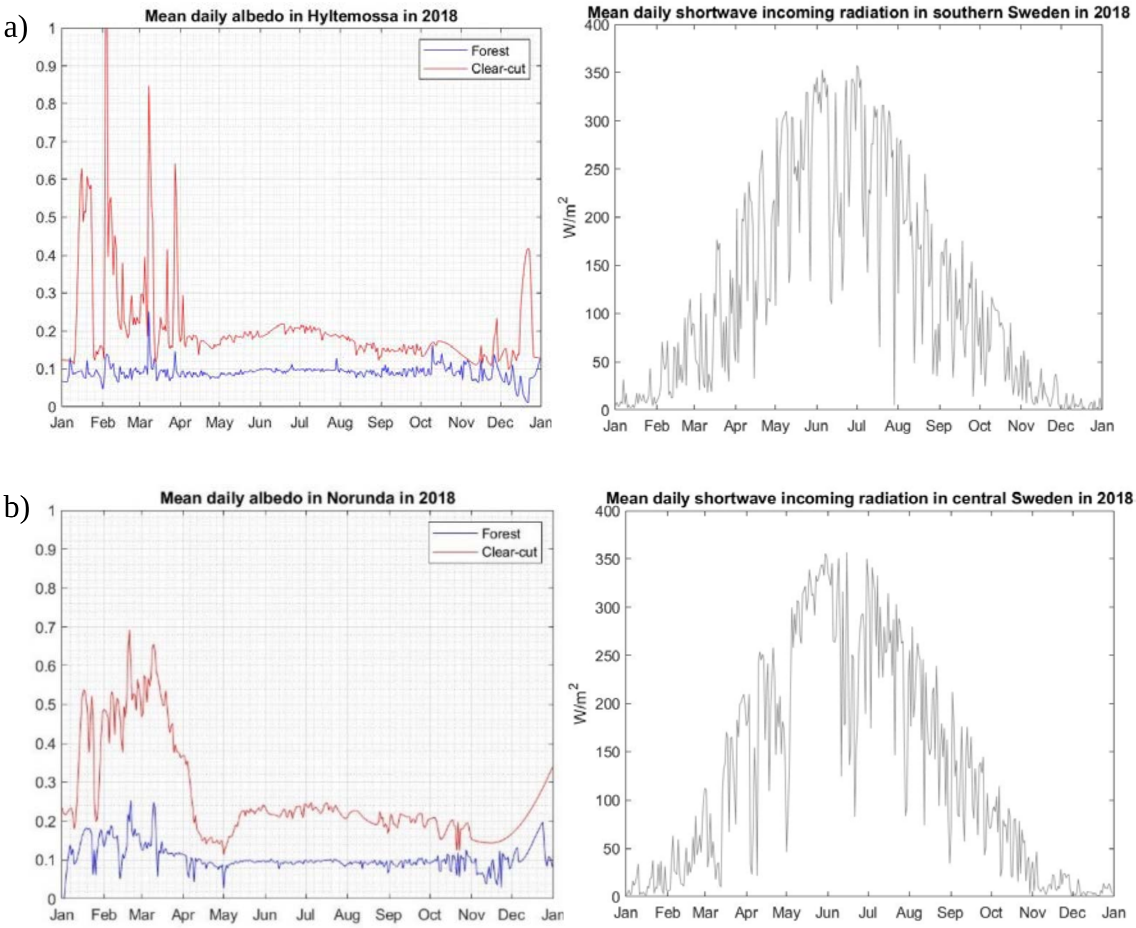

Figure 14. Comparison between the annual pattern of the mean daily albedo and mean daily SW_{in} in a) Hyltemossa and b) Norunda sites in 2018.

4.2 Radiative forcings by albedo change and by carbon dioxide release

Differences in radiative forcings by albedo change and by CO_2 release were compared and are shown in Table 7. Increase in $RF_{\Delta\alpha}$ by time at all latitudes is further illustrated in Figure 15.

Table 7. Comparison of radiative forcing by albedo change and radiative forcing by carbon dioxide release.

	$RF_{\Delta\alpha}$ (W/m^2_{Earth})	RF_{CO_2} (W/m^2_{Earth})	RF_{net} (W/m^2_{Earth})	$RF_{\Delta\alpha}/RF_{CO_2}$ (%)
Southern Sweden				
2016	-6.8×10^{-14}	12×10^{-14}	4.8×10^{-14}	59
2017	-7.3×10^{-14}		4.2×10^{-14}	63
2018	-8.0×10^{-14}		3.6×10^{-14}	69
Central Sweden				
2014	-6.4×10^{-14}	8.0×10^{-14}	1.6×10^{-14}	80
2015	-6.6×10^{-14}		1.4×10^{-14}	83
2016	-7.2×10^{-14}		0.8×10^{-14}	90
2017	-7.4×10^{-14}		0.6×10^{-14}	92
2018	-12×10^{-14}		-3.7×10^{-14}	146
Northern Sweden				
2014	-6.7×10^{-14}	4.3×10^{-14}	-2.4×10^{-14}	156

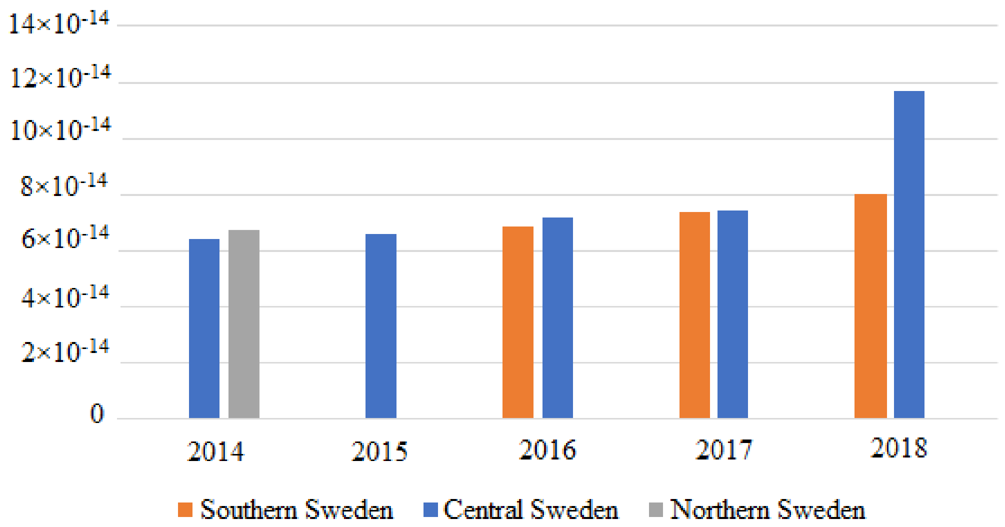

Figure 15. Radiative forcing by albedo change (W/m^2_{Earth}) at investigated sites.

The effect of RF_{net} at all examined latitudes is given in Table 8. and illustrated in Figure 16. Mean RF_{net} is positive in southern and central Sweden while it is negative in northern Sweden. The highest standard deviation of RF_{net} is in central Sweden where mean $RF_{\Delta\alpha}$ within the analysed time frame is almost equal to the RF_{CO_2} (98.1%).

Table 8. Net radiative forcing in southern, central and northern Sweden.

	Mean RF_{net} (W/m^2_{Earth})	St. deviation of RF_{net} (W/m^2_{Earth})	Mean $RF_{\Delta\alpha}/RF_{CO_2}$ (%)
Southern Sweden	4.2×10^{-14}	0.5×10^{-14}	63.9
Central Sweden	0.2×10^{-14}	1.9×10^{-14}	98.1
Northern Sweden	-2.4×10^{-14}	n. a.	156.2

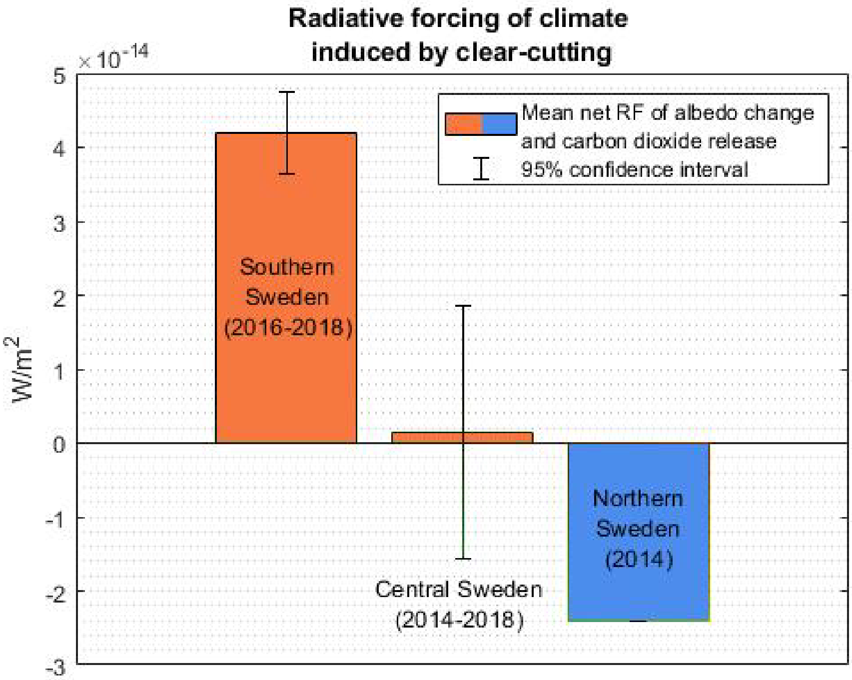

Figure 16. Mean net radiative forcing of clear-cutting in Sweden with a 95% confidence interval.

5. Discussion

5.1 Radiative flux

This study confirms analyses by Betts (2000) showing that the largest difference between mean annual albedo of different land surface types was in the farthest north. The mean annual albedo throughout the investigated period of a clear-cut area was higher than the one of a forest area by 59% in northern Sweden and by 57% in southern Sweden (Table 4). In addition, the study by Rost and Mayer (2006) conducted in south-western Germany (47°N), indicates that albedo of a grassland site was on average 52% higher than the one of the neighbouring sparse pine forest. The results are also in accordance to a study on albedo in the state New Hampshire in the USA (44°N) by Lutz and Howarth (2014) who showed that mean annual clear-cut albedo was on average 41% higher than the spruce-fir albedo (Table 9).

Table 9. Mean annual difference in albedo between clear-cuts and forests.

Study	Location	$\frac{\alpha^{\text{clear-cut}} - \alpha^{\text{forest}}}{\alpha^{\text{clear-cut}}}$ (%)
Mužić 2019	Sweden (56° - 64°N)	57 - 59
Rost and Mayer 2006	Germany (47°N)	52
Lutz and Howarth 2014	USA (44°N)	41

As illustrated in Figures 11 and 14, the difference between forest and clear-cut albedo is largest in the periods with snow presence. This is in accordance with studies by Betts (2000) and Stiller et al. (2005). The albedo of the forests never reaches the snow albedo values (0.45-0.95). Similar was found by Betts and Ball (1997) who illustrated that albedo of the coniferous forest sites in Saskatchewan and Manitoba in Canada (55°N) in winter rarely reaches 0.3. In the southern latitudes, there are fewer days with snow cover so the variations in albedo during winter days are higher what can be observed in single spikes in albedo in Figures 11 and 14. The mean summer albedo values in Hyltemossa sites are similar to the ones given by Betts and Ball (1997) (Table 10).

Table 10. Mean summer albedo in forests and clear-cuts.

Study	Location	Years	Mean summer α in the forest (-)	Mean summer α in the clear-cut (-)
Mužić 2019	Sweden (56°N)	2016 - 2018	0.09	0.19
Betts and Ball 1997	Canada (55°N)	1994 - 1995	0.08	0.20

The vegetation cover varies more in the clear-cuts than in forests during a year and has thus contributed to the larger change in albedo among various seasons in clear-cuts than in the forest areas (Table 5). Grasses in clear-cuts appear in early summer but they often become yellow and die out already in July. Therefore, summer albedo increases in mid-July to late July and then decreases from the beginning of August (Figures 11 and 14). Betts and Ball (1997) show that the mean summer albedo in grassland is 0.2, whereas it is 0.083 in the coniferous site which is slightly lower than presented in this study (Table 5). They also indicate that the jack pine sites and spruce sites have mean winter albedo of 0.15 and 0.11, respectively. This corresponds to the mean winter albedo values of forest sites investigated in this study.

Higher mean annual SW_{abs} in forest sites than in clear-cuts is a result of the difference in albedo between them since SW_{in} was similar on both sites (Table 6). The mean annual SW_{abs} throughout the examined periods of a forest site was higher than the one of a clear-cut site by 10-11% depending on latitude.

Within the same investigated year, the northern sites always had higher cumulative difference between the mean daily SW_{abs} in forests and clear-cuts because the longer daylight hours in the northern sites correspond to the summer period with high SW_{in} and because of a higher difference between albedo of the forests and clear-cuts in northern than in southern sites (Figure 13). At the beginning of 2014, the cumulative difference between the mean daily SW_{abs} in Svartberget and Degerö showed slower growth than the one between Norunda sites because of the longer darker period which decreased SW_{in} in the north. In spring, the cumulative difference between the mean daily SW_{abs} in Svartberget and Degerö had sharply increased surpassing the Norunda sites. The disparity between the two was the highest during spring because of an increase in number of daylight hours in northern sites and higher difference between albedos of the northern sites due to snow presence than in Norunda sites. In 2016, both mean annual albedo and mean annual SW_{in} were slightly higher in Norunda sites than in Hyltemossa sites as illustrated in Table 4. The cumulative difference between the mean daily SW_{abs} in Hyltemossa sites and Norunda sites started to deviate in spring 2016 due to longer daylight hours in central than in southern Sweden as well as due to higher albedo difference between Norunda sites than between Hyltemossa sites. In

2017, the cumulative differences overlapped throughout the whole year except at the end when the sites in Norunda had slightly higher values.

In 2018, the disparity among the cumulative difference between the mean daily SW_{abs} of Hyltemossa sites and the one between Norunda sites was considerably higher than in any of the previous years (Figure 13). The cumulative differences started to diverge from the end of winter and the disparity between them was the most prominent in the second half of the year. This happened because of the high SW_{in}, anomalous drought conditions and clear skies that year. The summer in Sweden in 2018 set new records in temperature, particularly in the south and central parts of the country. Warm, sunny and dry conditions prevailed in most of Sweden except in northern Norrland where there was a surplus in precipitation (SMHI 2018). High summer SW_{in} values and decreased cloud cover in May and at the beginning of June in Norunda can be observed in Figure 14. This goes in line with the finding that the largest ΔSW_{abs} between forest and clear-cut was in Norunda in 2018 (Table 6) as well as with the high mean annual SW_{in} and mean annual clear-cut albedo in Norunda in 2018 (Table 4). As a result, both high SW_{in} and clear-cut albedo contributed to the increase in mean annual SW_{abs} in Norunda sites in 2018.

An increase in summer albedo in clear-cuts each year (Table 5) has a higher contribution to a constant increase in $RF_{\Delta\alpha}$ by time (Figure 15) than small differences in winter albedo. This is because the snowfall in Sweden corresponds to the period with low SW_{in} (Sieber et al. 2019).

5.2 Carbon dioxide emission

Table 7 illustrates that RF_{co_2} decreased with increased latitude. The reason why RF_{co_2} decreases in the north of Sweden is because of the lower amount of above-ground biomass accounting for fewer trees per unit area than in the southern locations (Håkansson and Körling 2002). The carbon storage also differs depending on species type and is bigger in spruce than in pine forests (Akselsson et al. 2005).

5.3 Net radiative forcing

The net radiative forcing caused by clear-cutting (RF_{net}) decreased by time in both southern and central Sweden (Table 7). The reason for this might lie in the constant increase in $RF_{\Delta\alpha}$ due to the increase in summer albedo among years. However, this should be investigated in future studies. The outcome of the mean RF_{net} calculated in this study indicates different effects depending on the considered latitudes (Table 8 and Figure 16). Data on the mean RF_{net} suggests that clear-cutting in the southern and central Sweden has a warming effect on climate, whereas in northern Sweden it imposes cooling of the climate. RF_{net} was positive in Hyltemossa where, in comparison to other study sites, $RF_{\Delta\alpha}$ imposed the lowest proportion of the RF_{co_2}. Norunda had a positive RF_{net} in all years except in 2018 when $RF_{\Delta\alpha}$ became almost one and a half times higher than the RF_{co_2}. In Svartberget, however, $RF_{\Delta\alpha}$ was already more than one and a half times higher than RF_{co_2}in 2014.

The highest uncertainty imposes the climatic effect of changes in RF_{net} due to clear-cutting in the two northern sites. The net effect in central Sweden, a site with the longest time series, showed very high variability among different years. The net response of climate to clear-cutting in northern Sweden is based on the single year data which is considered insufficient for determining the general pattern. Furthermore, RF_{co_2} was calculated as a time-independent variable and does not correspond to the same years as the data on SW_{abs} (Bright et al. 2016). In addition, post-harvest changes in CO_2 fluxes were not considered. Moreover, the contribution of $RF_{\Delta\alpha}$ and $RF_{co_2}$to RF_{net} may not change linearly in time. Albedo can abruptly decrease throughout the development of forest by modifications in the canopy density, while changes in the carbon storage happen more slowly (Betts 2000). Warm, sunny and dry conditions, as in the case of Norunda sites in 2018, also have an influence on RF_{net} (Table 7). Therefore, more years of available instrumental data on radiation and CO_2 fluxes are needed to provide a comparison of the results in various study sites (with different soil properties, weather events, insect infestations, etc.) for a longer continuous time period during the whole rotation cycle of a forest. As a result, based on the data used in this study, with a 95% confidence interval it is not possible to claim if clear-cutting induces warming or cooling what is particularly unclear in central and northern Sweden.

5.4 Effect of land-use change in high-latitudes in the future

The RF_{net} of land-use to the climate in the future is unknown. The outcome of the complex interactions between the forests and climate will depend on the magnitude of climate change. Modifications in the atmospheric CO_2 concentration, temperature or precipitation could have a substantial impact on the properties of the forests which could then, in turn, affect climate.

Associated with the growing demand for the forest products, policy makers have developed various forest management programs which aim to increase the carbon sequestration of the forests and reduce atmospheric greenhouse gas concentrations.

These include afforestation and conversion of natural forests to plantations (Gower 2003). Even though the management practices can increase the carbon sequestration rates by ensuring that there is the sufficient nutrient and water availability, each forest region has a threshold representing maximum sequestration potential and shows a different response to the added substances. For example, irrigation and nitrogen fertilisation have reinforced the carbon sink of the Scots pine (Pinus sylvestris) in southern Sweden by 78% (Gower 2003). From the albedo point of view, it is suggested to increase the number of broadleaved trees in the coniferous forests in order to maximize albedo of the boreal forest areas. In that way, boreal forests would absorb less incoming radiation but will not show a decrease in productivity (Hovi et al. 2016). However, not all forest management practices mitigate climate change (Naudts et al. 2016). Almost all studies that estimate the carbon sequestration potential account only for the carbon accumulation in trees thereby neglecting the carbon accumulation in ground vegetation (Vesala et al. 2005; Lindroth et al. 2018). Equally important, most studies do not account for carbon emissions from harvest and mills as well as the transportation emissions to processing plants, regional distributors or consumers. Similarly, greenhouse gas emissions associated with the production of fertilisers are often disregarded (Gower 2003). Finally, most of the studies examining forest management practices focus on the increase of carbon storage and thereby neglect the albedo effect.

5.5 Potential improvements

In the study, some of the contributing factors were disregarded to lower the complexity of various processes. Future studies should thus account for a larger complexity of the interactions among the involved factors. These should examine the annual pattern of the vegetation growth in clear-cuts which would explain why summer albedo in clear-cuts increases among years contributing to an increase in $RF_{\Delta\alpha}$. Soil properties of investigated sites, as well as weather components such as air temperature, humidity, wind speed, wind direction, soil heat flux, soil moisture and precipitation, should be incorporated to examine their interdependence with a change in the RF_{net}. This would also show how atmospheric circulation might affect distant regional climates. A major improvement not requiring a global (or regional) climate/biogeophysical modelling approach would be to take into account the CO_2 fluxes after clear-cut was established. Furthermore, adopting data on annual net cumulative CO_2 flux derived from eddy-covariance measurements in clear-cuts for calculation of RF_{CO_2} would enable direct comparison with the radiation fluxes at different sites for the same years. The utilisation of data on both albedo change as well as on CO_2 emission in clear-cuts during the whole rotation cycle of the managed forests would provide a more accurate evaluation of the climatic effect from clear-cutting. Finally, including emissions from not only CO_2 but also other greenhouse gases such as CH_4 and N_2O following clear-cutting would contribute to the accuracy of the results (Vestin 2017).

6. Conclusion

Previous studies illustrate that the land surface modifications have a capacity to affect climatic conditions through the changes in albedo and greenhouse gas concentration. The results varied in magnitude of change depending on the spatial location of the investigated area.

In this study, the net effect of clear-cutting on climate was examined on three latitudes in Sweden to account for the different temperature, length of the incoming radiation, moisture availability, etc. in those areas. The analysis was performed by comparing the $RF_{\Delta\alpha}$ in the forest and clear-cut study site pairs and RF_{CO_2} from clear-cutting.

The outcome of the comparison between the forest and clear-cut sites on the same latitudes confirmed previous studies showing that the albedo of the clear-cut was higher than the forest albedo and that the mean annual SW_{abs} in the forest was higher than that of the clear-cut in all $RF_{\Delta\alpha}$ examined years and at all latitudes.

The results comparing the effect at different latitudes supported previous studies illustrating that $RF_{\Delta\alpha}$ increases with increased latitude when comparing the same years. It has also been shown that RF_{co_2} decreases with increased latitude.

In southern Sweden (56°N), the mean RF_{net} due to clear-cutting had a net warming effect on climate during all years in the investigated period, between 2016 and 2018. In central Sweden (60°N), the mean RF_{net} due to clear-cutting had a net warming effect on climate in the period between 2014 and 2018. However, the $RF_{\Delta\alpha}$ was nearly equal to the RF_{co_2} in all years except in 2018 when it overweighed the latter. Therefore, clear-cutting had a net warming effect on the climate in all years except in 2018. In northern Sweden (64°N), the RF_{net} due to clear-cutting had a net cooling effect on climate in 2014.

To conclude, the outcome of clear-cutting to climate varies considerably depending on the latitudinal position of the examined sites. This may indicate that the climatic conditions have an important role in the RF_{net} by land-use change. Based on the provided results, clear-cutting in the southern and central Sweden has a warming effect on climate whereas the same process imposes cooling in northern Sweden. This study underlines results from the previous research, illustrates the importance of the climatic conditions to the changes in albedo and CO_2 and provides an insight into the climatic effect of $RF_{\Delta\alpha}$ and RF_{co_2} in the Swedish context. It also implies that the albedo effect has an essential role in the estimation of the climatic effect of clear-cutting and should thus be incorporated in future forest management strategies. Due to a lack of data, the outcome of this stand-alone study is not able to support the hypothesis that the high-latitude clear-cutting can reduce climate warming with a high level of confidence.

References

Akselsson, C., B. Berg, V. Meentemeyer, and O. Westling. 2005. Carbon sequestration rates in organic layers of boreal and temperate forest soils - Sweden as a case study. *Global Ecology and Biogeography* 14: 77–84. doi:10.1111/j.1466-822X.2004.00133.x.

Archer, D. 2010. *The Global Carbon Cycle*. Princeton: Princeton University Press.

Bergvik Skog. 2019. *Life Cycle of a Forest*. Retrieved 12 May 2019, from https://www.bergvikskog.se/en/forest-land-water/forestry/life-cycle-of-a-forest/.

Betts, A., and J. Ball. 1997. Albedo over the boreal forest. *Journal of Geophysical Research: Atmospheres* 102: 28901-28909. American Geophysical Union (AGU). doi:10.1029/96jd03876.Betts, R. A. 2000. Offset of the potential carbon sink from boreal forestation by decreases in surface albedo. *Nature* 408: 187–190. doi:10.1038/35041545.

Betts, R. A. 2001. Biogeophysical impacts of land use on present-day climate: Near-surface temperature change and radiative forcing. *Atmospheric Science Letters* 2: 39–51. doi:10.1006/asle.2001.0023.

Bounoua, L., R. DeFries, G. J. Collatz, P. Sellers, and H. Khan. 2002. Effects of land cover conversion on surface climate. *Climatic Change* 52: 29–64. doi:10.1023/A:1013051420309.

Bright, R. M., W. Bogren, P. Bernier, and R. Astrup. 2016. Carbon-equivalent metrics for albedo changes in land management contexts: Relevance of the time dimension. *Ecological Applications* 26: 1868–1880. doi:10.1890/15-1597.1.

Chapin, F. S., M. Sturm, M. C. Serreze, J. P. McFadden, J. R. Key, A. H. Lloyd, A. D. McGuire, T. S. Rupp, et al. 2005. Role of land-surface changes in arctic summer warming. *Science* 310: 657–660. doi:10.1126/science.1117368.

Ciais, P., C. Sabine, G. Bala, L. Bopp, V. Brovkin, J. Canadell, A. Chhabra, R. DeFries, J. Galloway, M. Heimann, C. Jones, C. Le Quéré, R.B. Myneni, S. Piao and P. Thornton, 2013: Carbon and Other Biogeochemical Cycles. In: Cli- mate Change 2013: The Physical Science Basis. Contribution of Working Group I to the Fifth Assessment Report of the Intergovernmental Panel on Climate Change [Stocker, T.F., D. Qin, G.-K. Plattner, M. Tignor, S.K. Allen, J. Boschung, A. Nauels, Y. Xia, V. Bex and P.M. Midgley (eds.)]. Cambridge University Press, Cambridge, United Kingdom and New York, NY, USA.

Claussen, M., V. Brovkin, and A. Ganopolski. 2001. Biogeophysical versus biogeochemical feedbacks of large-scale land cover change. *Geophysical Research Letters* 28: 1011-1014. American Geophysical Union (AGU). doi:10.1029/2000gl012471.

Earth’s CO_2. 2019. Retrieved 6 May 2019, from https://www.co2.earth/.

Google Earth. 2019a. *ICOS Hyltemossa.* Retrieved 29 March 2019, from https://earth.google.com/web/@56.10014388,13.41675567,118.01676276a,1814.18116179d,35y,0h,0t,0r.

Google Earth. 2019b. *ICOS Norunda,* Retrieved 29 March 2019, from https://earth.google.com/web/@60.08357997,17.47436145,72.76878488a,3140.86731999d,35y,0h,0t,0r.

Gordon, B. B. 2008. Forests and Climate Change: Forcings, Feedbacks, and the Climate Benefits of Forests. *Science* 320: 1444.

Gower, S. T. 2003. PATTERNS AND MECHANISMS OF THE FOREST CARBON CYCLE. *Annual Review of Environment and Resources* 28: 169–204. doi:10.1146/annurev.energy.28.050302.105515.

Håkansson, J., and A. Körling. 2002. Uppskattning av mängden kol i trädform: en metodstudie. *Lunds universitets Naturgeografiska institution - Seminarieuppsatser.* (in Swedish, English summary)

Houghton, J. 2009. *Global warming*. Cambridge: Cambridge University Press.

Hovi, A., J. Liang, L. Korhonen, H. Kobayashi, and M. Rautiainen. 2016. Quantifying the missing link between forest albedo and productivity in the boreal zone. *Biogeosciences* 13: 6015–6030. doi:10.5194/bg-13-6015-2016.

ICOS Carbon Portal Data. 2019. *ICOS RI, licensed under CC4BY*. Retrieved 6 May 2019, from https://www.icos-cp.eu/data.

ICOS Sweden. 2019a. *Data*, Retrieved 29 March 2019, from http://www.icos-sweden.se/data.html.

ICOS Sweden. 2019b. *Network and Measurements,* Retrieved 28 March 2019, from http://www.icos-sweden.se/station.html.

IPCC, 2014a: Annex II: Glossary [Mach, K.J., S. Planton and C. von Stechow (eds.)]. In: Climate Change 2014: Synthesis Report. Contribution of Working Groups I, II and III to the Fifth Assessment Report of the Intergovernmental Panel on Climate Change [Core Writing Team, R.K. Pachauri and L.A. Meyer (eds.)]. IPCC, Geneva, Switzerland, pp. 117-130.

IPCC, 2014b: Climate Change 2014: Synthesis Report. Contribution of Working Groups I, II and III to the Fifth Assessment Report of the Intergovernmental Panel on Climate Change [Core Writing Team, R.K. Pachauri and L.A. Meyer (eds.)]. IPCC, Geneva, Switzerland, 151 pp.

Keenan, R. J., G. A. Reams, F. Achard, J. V. de Freitas, A. Grainger, and E. Lindquist. 2015. Dynamics of global forest area: Results from the FAO Global Forest Resources Assessment 2015. *Forest Ecology and Management* 352. Elsevier B.V.: 9–20. doi:10.1016/j.foreco.2015.06.014.

Kiehl, J. T., and K. E. Trenberth. 1997. Earth's Annual Global Mean Energy Budget. *Bulletin of the American Meteorological Society* 78: 197–208. doi:10.1175/1520-0477(1997)078<0197:EAGMEB>2.0.CO;2.

Kipp & Zonen. 2019. Retrieved 4 April 2019, from https://www.kippzonen.com/Product/85/CNR4-NetRadiometer#.XKWkC5gzbMV.

Lindroth, A., J. Holst, M. Heliasz, P. Vestin, F. Lagergren, T. Biermann, Z. Cai, and M. Mölder. 2018. Effects of low thinning on carbon dioxide fluxes in a mixed hemiboreal forest. *Agricultural and Forest Meteorology* 262: 59–70. doi:10.1016/j.agrformet.2018.06.021.

Lutz, D. A., and R. B. Howarth. 2014. Valuing albedo as an ecosystem service: Implications for forest management. *Climatic Change* 124: 53–63. doi:10.1007/s10584-014-1109-0.

Luyssaert, S., E. Schulze, A. Börner, A. Knohl, D. Hessenmöller, B. Law, P. Ciais, and J. Grace. 2008. Old-growth forests as global carbon sinks. *Nature* 455: 213-215. Springer Science and Business Media LLC. doi:10.1038/nature07276.Krinner, G. 2003. Impact of lakes and wetlands on boreal climate. *Journal of Geophysical Research* 108. doi:10.1029/2002jd002597.

Luyssaert, S., M. Jammet, P. C. Stoy, S. Estel, J. Pongratz, E. Ceschia, G. Churkina, A. Don, et al. 2014. Land management and land-cover change have impacts of similar magnitude on surface temperature. *Nature Climate Change* 4: 389–393. doi:10.1038/nclimate2196.

Luyssaert, S., G. Marie, A. Valade, Y. Y. Chen, S. Njakou Djomo, J. Ryder, J. Otto, K. Naudts, et al. 2018. Trade-offs in using European forests to meet climate objectives. *Nature* 562. Springer US: 259–262. doi:10.1038/s41586-018-0577-1.

Mamkin, V., J. Kurbatova, V. Avilov, D. Ivanov, O. Kuricheva, V. Andrej, I. Yaseneva, and A. Olchev. 2019. Energy and CO2 exchange in an undisturbed spruce forest and clear-cut in the Southern Taiga. *Agricultural and Forest Meteorology* 265. Elsevier: 252–268. doi:10.1016/j.agrformet.2018.11.018.

Marklund, L. G., 1988. Biomass functions for pine, spruce and birch in Sweden. Report 45. Department of Forest Survey, Swedish University of Agricultural Sciences, Umeå, Sweden.

Moene, A. F., and J. C. van Dam. 2013. *Transport in the Atmosphere-Vegetation-Soil Continuum*. Cambridge: Cambridge University Press.

Monteith, J. L., and M. H. Unsworth. 2013. *5 Radiation Environment. Principles of Environmental Physics (Fourth Edition)*. doi:10.1016/B978-0-12-386910-4.00005-6.

Myhre, G., and A. Myhre. 2003. Uncertainties in radiative forcing due to surface Albedo changes caused by land-use changes. *Journal of Climate* 16: 1511–1524. doi:10.1175/1520-0442-16.10.1511.

Myhre, G., D. Shindell, F.-M. Bréon, W. Collins, J. Fuglestvedt, J. Huang, D. Koch, J.-F. Lamarque, et al. 2013. *Anthropogenic and Natural Radiative Forcing*.

Nabuurs, G. J., and G. M. J. Mohren. 1995. Modelling analysis of potential carbon sequestration in selected forest types. *Canadian Journal of Forest Research* 25: 1157–1172. doi:10.1139/x95-128.

Naudts, K., Y. Chen, M. McGrath, J. Ryder, A. Valade, J. Otto, and S. Luyssaert. 2016. Europes forest management did not mitigate climate warming. *Science* 351: 597-600. American Association for the Advancement of Science (AAAS). doi:10.1126/science.aad7270.

Nilsson, S., and W. Schopfhauser. 1995. The carbon-sequestration potential of a global afforestation program. *Climatic Change* 30: 267–293. doi:10.1007/BF01091928.

Pitman, A. 2003. The evolution of, and revolution in, land surface schemes designed for climate models. *International Journal of Climatology* 23: 479-510. Wiley. doi:10.1002/joc.893.Quéré, C., R. Andrew, P. Friedlingstein, S. Sitch, J. Hauck, J. 51

Pongratz, P. Pickers, J. Ivar Korsbakken, et al. 2018. Global Carbon Budget 2018. *Earth System Science Data* 10: 2141–2194. doi:10.5194/essd-10-2141-2018.

Roe, G. 2009. Feedbacks, Timescales, and Seeing Red. *Annual Review of Earth and Planetary Sciences* 37: 93–115. doi:10.1146/annurev.earth.061008.134734.

Rost, J., and H. Mayer. 2006. Comparative analysis of albedo and surface energy balance of a grassland site and an adjacent Scots pine forest. *Climate Research* 30: 227–237.

Roupsard, O., A. Black, A. Lindroth, R. Steinbrecher, A. R. Desai, S. Besnard, N. Carvalhais, M. Jung, et al. 2018. Quantifying the effect of forest age in annual net forest carbon balance. *Environmental Research Letters* 13. IOP Publishing: 124018. doi:10.1088/1748-9326/aaeaeb.

Sathre, R., and L. Gustavsson. 2012. Time-dependent radiative forcing effects of forest fertilization and biomass substitution. *Biogeochemistry* 109: 203–218. doi:10.1007/s10533-011-9620-0.

Sieber, P., N. Ericsson, and P. Hansson. 2019. Climate impact of surface albedo change in Life Cycle Assessment: Implications of site and time dependence. *Environmental Impact Assessment Review* 77: 191-200. Elsevier BV. doi:10.1016/j.eiar.2019.04.003.

SkogsSverige. 2016. *Omföringstabell vanliga kubikmetermått i skogen.* [Conversion table ordinary cubic meter measurements in the forest. In Swedish]. Retrieved 6 May 2019, from https://www.skogssverige.se/omvandlare.

SMHI. 2018. *Sommaren 2018 - Extremt varm och solig*. [Summer 2018 - Extremely warm and sunny. In Swedish]. Retrieved 13 May 2019, from https://www.smhi.se/klimat/klimatet-da-och-nu/arets-vader/sommaren-2018-extremt-varm-och-solig-1.138134.

Stewart, J. 1971. The albedo of a pine forest. *Quarterly Journal of the Royal Meteorological Society* 97: 561-564. Wiley. doi:10.1002/qj.49709741417.Stiller, B., F. Beyrich, G. Hollaz, J. P. Leps, S. Richter, and U. Weisensee. 2005. Continuous measurements of the energy budget components at a pine forest and at a grassland site. *Meteorologische Zeitschrift* 14: 137–142. doi:10.1127/0941-2948/2005/0014.

Swedish Environmental Protection Agency. 2018. *Swedish national inventory report 2018*. *Naturvårdsverket*.

The Scientific American science desk reference. 1999. New York: John Wiley.

UNFCCC. 2015. *ADOPTION OF THE PARIS AGREEMENT - Paris Agreement text English*.

Vashum, K. T. 2012. Methods to Estimate Above-Ground Biomass and Carbon Stock in Natural Forests - A Review. *Journal of Ecosystem & Ecography* 02. doi:10.4172/2157-7625.1000116.

Vesala, T., T. Suni, Ü. Rannik, P. Keronen, T. Markkanen, S. Sevanto., T. Grönholm, S. Smolander, et al. 2005. Effect of thinning on surface fluxes in a boreal forest. *Global Biogeochemical Cycles* 19: 1–11. doi:10.1029/2004GB002316.

Vestin, P. 2017. Effects of forest management on greenhouse gas fluxes in a boreal forest. PhD Thesis. Lund University.

Wallerman, J., J. Bohlin, M. B. Nilsson, and J. E. S. Fransson. 2018. DRONE-BASED FOREST VARIABLES MAPPING OF ICOS TOWER SURROUNDINGS Swedish University of Agricultural Sciences, Dept. of Forest Resource Management , Umeå , Sweden Swedish University of Agricultural Sciences , Dept. of Forest Ecology and Management, Umeå: 9003–9006.